

AD-A111 175

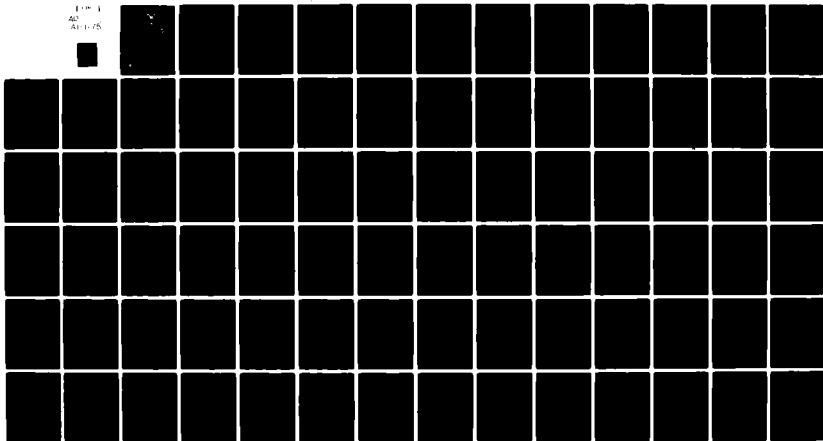
AIR FORCE INST OF TECH WRIGHT-PATTERSON AFB OH SCHOO--ETC F/8 20/5  
SPECTROSCOPIC ANALYSIS OF PBO CHEMILUMINESCENCE.(U)  
DEC 81

UNCLASSIFIED

AFIT/SEP/PH/81D-9

NL

175-1  
AD-A111-175



END

DATE

FILED

3-82

DTIC

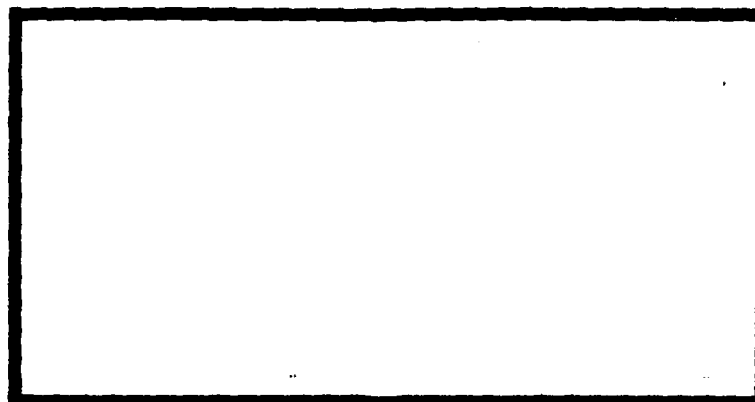
AD A111175



LEVEL II

①

DTIC  
ELECTE  
S FEB 19 1982 D  
E



UNITED STATES AIR FORCE  
AIR UNIVERSITY  
AIR FORCE INSTITUTE OF TECHNOLOGY  
Wright-Patterson Air Force Base, Ohio

DTIC FILE COPY

This document has been approved  
for public release and sale; its  
distribution is unlimited.

82 02 18 066

AFIT/GEP/PH/81D-9

LEVEL II (1)

SPECTROSCOPIC ANALYSIS  
OF PbO CHEMILUMINESCENCE

THESIS

AFIT/GEP/PH/81D-9

Steven R. Snyder  
1Lt USAF

Approved for public release; distribution unlimited.

SPECTROSCOPIC ANALYSIS  
OF PbO CHEMILUMINESCENCE

THESIS

Presented to the faculty of the School of Engineering  
of the Air Force Institute of Technology  
Air University  
in Partial Fulfillment of the  
Requirements for the Degree of  
Master of Science

Accession For	
NTIS GPO	<input checked="checked" type="checkbox"/>
DTIC TAB	<input type="checkbox"/>
Unannounced	<input type="checkbox"/>
Justification	<input type="checkbox"/>
Re-	
File	<input type="checkbox"/>
Availability	<input type="checkbox"/>
Dist	<input type="checkbox"/>
A	<input type="checkbox"/>

by

Steven R. Snyder, B.S.

1Lt

USAF

Graduate Engineering Physics

October 1981

Approved for public release; distribution unlimited

## Preface

The motivation for this thesis is due to the Air Force's interest in chemical lasers. Knowledge gained from this research will provide the Air Force Weapons Laboratory with data which will indicate possible directions to follow in chemical laser development. I personally chose this thesis topic because of a keen interest in both laser theory and spectroscopy.

I wish to thank Dr. Steve Davis for providing some of the equipment used in this research and Dr. E. A. Dorko, my advisor, for his support in preparing this manuscript. I would also like to thank my wife, Linda, for her patience with my efforts.

Steven R. Snyder

## Contents

	<u>Page</u>
Preface.....	ii
List of Figures.....	v
List of Tables.....	vi
Abstract.....	vii
I. Introduction.....	1
Background.....	1
Problem.....	2
General Approach.....	2
II. Theory.....	3
Introduction.....	3
Coupling.....	3
Spectra.....	10
Reaction Exothermicities.....	15
Background.....	16
III. Experimental Apparatus.....	21
Introduction.....	21
Set-Up.....	21
Flow Tube Modifications.....	24
IV. Experimental Procedure.....	27
Introduction.....	27
General Procedures.....	27
Alignment.....	28
Calibration.....	29
Noise Reduction.....	29
V. Results and Discussion.....	31
Flow Tube Performance and Experimental Observations... 31	
Spectra and Assignments.....	32
Variation of Oxidizer Pressure.....	40
VI. Conclusions and Recommendations.....	51
Excited Gases.....	52
Flow Tube.....	52
Chimney Design.....	52
Oxidizer Injection.....	52
Bibliography.....	54

## Contents

	<u>Page</u>
Appendix A: Grating Response Curve.....	56
Appendix B: Photomultiplier Response Curve.....	57
Appendix C: Representative Spectra.....	59
Appendix D: Pb + N <sub>2</sub> O Pressure Variation Spectra.....	65
Vita.....	71

## List of Figures

<u>Figure</u>		<u>Page</u>
1	Hund's Coupling Cases.....	4
2	P <sup>2</sup> Energy Correlation Diagram.....	6
3	Emission Lines of Pb.....	7
4	Correlation Diagram for PbO.....	11
5	Potential Curves.....	12
6	PbO Spectrum Showing Bandheads.....	14
7	Energies of States and Reaction Exothermicities.....	17
8	Intensity Ratio Plots.....	19
9	Experimental Set-up.....	22
10	Furnace and Reaction Area.....	23
11	Gas curtain.....	26
12	Spectrum of Pb + N <sub>2</sub> O Reaction.....	34
13	Spectrum of Pb + O <sub>2</sub> Reaction.....	35
14	Pb + O <sub>2</sub> Spectra with Oxidizer Variation.....	41
15	Pb + O <sub>2</sub> Intensity Ratio Plot.....	47
16	Pb + N <sub>2</sub> O Intensity Ratio Plot.....	50
17	Proposed Experimental Configuration.....	53



# List of Tables

<u>Table</u>		<u>Page</u>
I	Emission Lines of PbO.....	1
II	Molecular orbitals and Spectroscopic Terms.....	9
III	Separated Atom States and $\Omega$ Values .....	9
IV	Heats of Formation.....	15
V	Reactions and Exothermicities.....	16
VI	Band Heads of the Pb + N <sub>2</sub> O Reaction.....	36
VII	Band Heads of the Pb + O <sub>2</sub> Reaction.....	38

# ABSTRACT

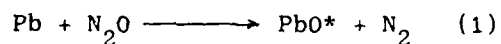
A lead oxide (PbO) flame was generated in a flow tube reactor by reacting lead vapor generated in a furnace with the oxidizers  $O_2$  and  $N_2O$ . The emissions from the chemiluminescent flames were analyzed by means of a Jarrell-Ash 0.25 m spectrograph and photomultiplier operating in the region 2000-8000 Å. Rovibronic bands assignable to the x-a, x-b, x-A, x-B electronic systems were observed. The assignments compare well with published work. Spectra obtained with the two different oxidizers were compared. Significant differences in spectral line intensities were recorded. The pressure dependence of the intensities was also measured. Again, significant differences were recorded when the two different oxidizers were used. In the  $Pb + O_2$  reaction a low pressure enhancement of various lines was observed. Significant differences between the chemistry of these low pressure reactions and the chemistry of similar reactions of high pressure were observed.

# SPECTROSCOPIC ANALYSIS OF PbO CHEMILUMINESCENCE

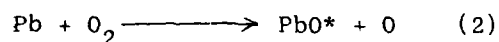
## I. Introduction

### Background

A chemical electronic transition laser (CETL) uses a chemical reaction to produce the lasing species. Consequently, the scale-up of such systems is not inhibited by the presence of large and heavy electrical power supplies (Ref 12:2). For this reason CETL's are attractive candidates for military laser systems. Two reactions which could be the basis for a CETL are,



and,



where the \* indicates that the lead oxide molecule is produced in an electronically excited state. In lead oxide, emission is observed from six different excited electronic states. These are shown in Table I. The extent to which the various electronic states are populated by the above reactions depends on temperature,

TABLE I  
Emission Lines of PbO<sup>1</sup>

<u>TRANSITION</u>	<u><math>\bar{\nu}_{00} (\text{cm}^{-1})</math></u> <sup>2</sup>	<u><math>\lambda (\text{\AA})</math></u> <sup>0</sup>
E $\longrightarrow$ X	34,755.0	2877.3
D $\longrightarrow$ X	30,103.2	3321.9
B $\longrightarrow$ X	22,173.4	4509.9
A $\longrightarrow$ X	19,728.3	5068.9
b $\longrightarrow$ x	16,175.7	6182.1
a $\longrightarrow$ X	15,905.3	6287.2

1. All transitions shade toward red
2. Values taken from various literature sources

oxidizer pressure, and the reaction exothermicity. A study of reactions (1) and (2) at different oxidizer pressures forms the basis for this thesis.

#### Problem

The purpose of this research was to determine how the chemiluminescent emission produced in reactions (1) and (2) would change as oxidizer pressure was varied. Chemiluminescence is the radiation given off from those reaction products which are produced in an excited state.

In addition, certain modifications were made to experimental equipment to increase signal strength and to prevent reaction products from collecting on observation windows. The detection system, although conventional in nature, had not previously been used to detect chemiluminescent signals from lead oxide. Therefore, the detection system was optimized.

#### General Approach

A gas flow tube reactor was used to generate the chemiluminescent reactions. It was important that the observed spectra be generated by a chemiluminescent means as this would more closely correspond to the actual conditions in a CETL. Lead vapor was entrained in argon gas and carried to the flow tube reaction region where the oxidizers were introduced. The resulting chemiluminescent flame was then spectroscopically analyzed in a conventional manner. The dependence of spectra on oxidizer pressure was examined.

## II. Theory

### Introduction

In this chapter the theory relating to the spectroscopy of lead oxide ( $\text{PbO}$ ) will be discussed. First, a discussion of the two pertinent angular momentum coupling schemes, Hunds' cases a and c (Ref 2), will be presented, and second, a detailed analysis will show a correlation between the various excited states of the separated atoms and the excited states of the  $\text{PbO}$  molecule. Next, there will be a brief discussion on the type of spectra observed from electronically excited diatomic molecules. The exothermicity of lead-oxidizer reactions will be examined to determine which electronic states of lead oxide should be observed with each oxidizer. Finally, a summary of previous work on lead oxide will be given.

### Coupling

In lead oxide, where the ground state is  $^1\Sigma$ , two angular momentum coupling schemes are possible. These are Hunds' cases a and c. Both cases describe the manner in which  $L$ , the orbital angular momentum, and  $S$ , the spin angular momentum, are coupled in the molecule to form  $J$ , the total angular momentum. In case a both  $L$  and  $S$  are coupled individually to the internuclear axis; see Figure 1. The sum of their projections on the internuclear axis,  $\Lambda$  and  $\Sigma$ , respectively, then forms,  $\Omega$ , the total angular momentum without rotation.  $N$ , the rotational angular momentum of the molecule, is then coupled with  $\Omega$  to form  $J$ , the total angular momentum of the molecule. In case c,  $L$  and  $S$  are first coupled with each other to form a  $J'$ . The projection of  $J'$  on the internuclear axis is then  $\Omega$ .  $\Omega$  and  $N$  are then coupled to form  $J$ , the total angular momentum of the molecule. The two cases are shown pictorially in Figure 1. In most molecules, case a coupling is the dominant feature, but for heavy molecules case c coupling may play an important role. This should be expected since the

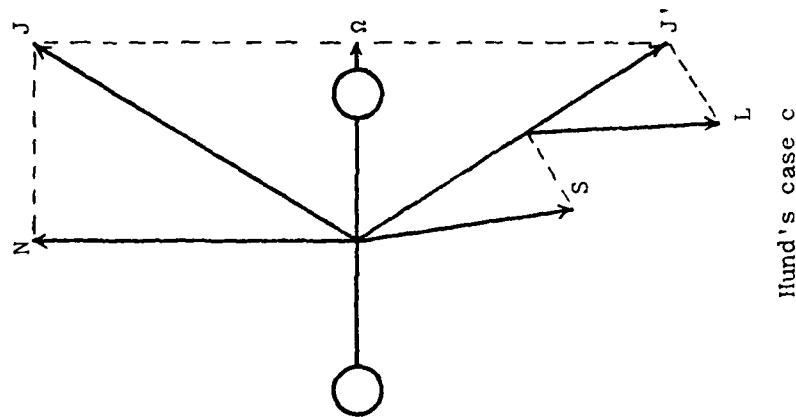
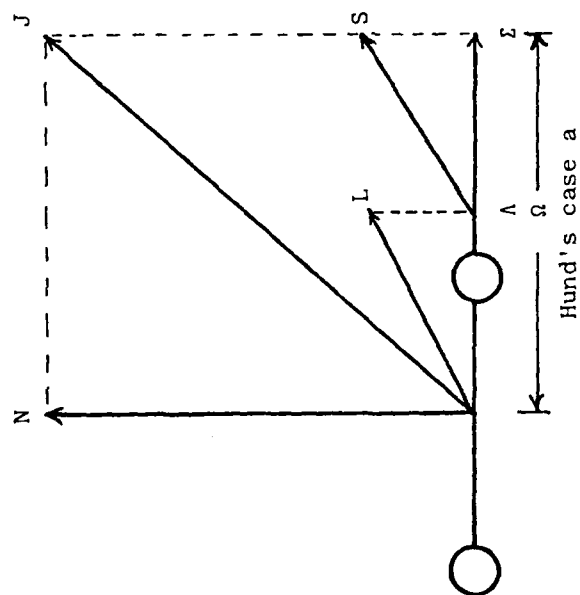


Figure 1 Hund's Coupling Cases

electrons in very heavy molecules are farther from the nuclei than they are in lighter molecules and, hence, can more easily interact with each other than they can with the two nuclei. (Ref 2)

Molecules with predominant case c coupling would arise from heavy atoms obeying j-j coupling (j-j coupling is the single atom analog of case c molecular coupling). Therefore lead oxide should only be treated as case c if lead follows the j-j coupling scheme for single atoms.

Lead has  $6S^2 6P^2$  for its outer shell electronic arrangement. This leads to a  $P^2$  configuration which can be shown spectroscopically in an energy correlation diagram; see Figure 2. This diagram shows how the energy states are changed or split up as the electron correlation and spin orbit effects are taken into account. Column 3 in Figure 2 shows the correct order that the spectroscopic states would fall in if the atom obeys L-S coupling (single atom analog of case a). Column 4 shows the ordering of the states if the atom obeys j-j coupling. As shown, states in j-j coupling are designated by their J values since L and S no longer lead to valid quantum numbers. As can be seen in Figure 2 the large spin-orbit coupling in j-j coupling results in a large splitting of the triplet states. So great is this splitting that two of the triplet states may actually occur above the  $^1S$  state, and emission from the triplet state will actually be observed as emission from three separate electronic states, selection rules being favorable. The extent to which lead oxide will be either case a or case c can be inferred by correlating the observed lead emission lines with the positions of the spectroscopic states as shown in Figure 2. The observed emission lines of lead and their spectroscopic designations are given in Figure 3. As shown, the three triplet states are split apart (denotes j-j coupling), but the states occur in

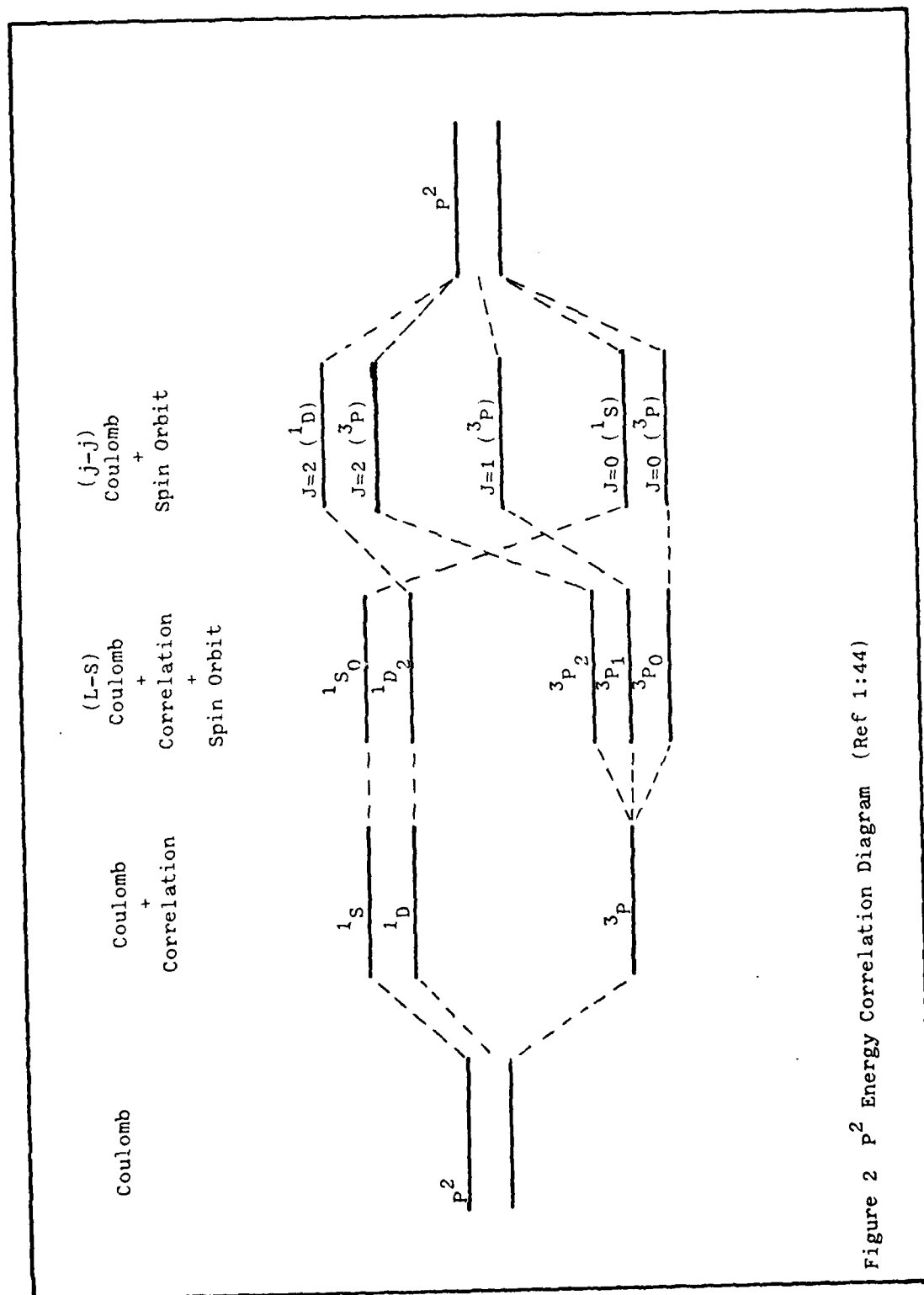


Figure 2  $p^2$  Energy Correlation Diagram (Ref 1:44)



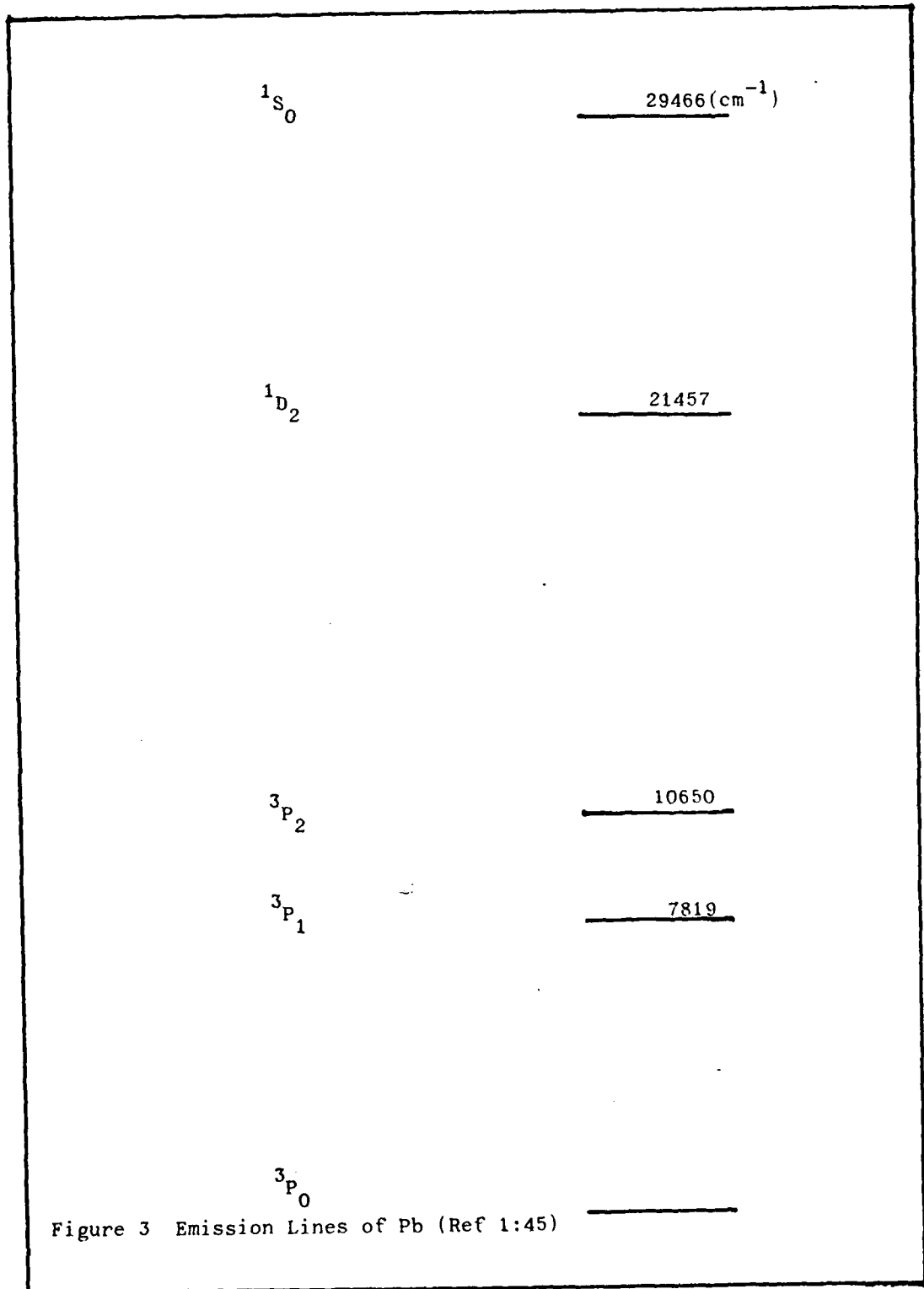


Figure 3 Emission Lines of Pb (Ref 1:45)

in the order which corresponds to L-S coupling. Therefore, even though lead oxide is a relatively heavy molecule and does experience some amount of case c coupling, it can still be treated as case a for spectroscopic purposes. It should be pointed out that the above analysis is for lead oxide in the ground state only. It is possible for some excited state to exhibit strong case c coupling. Indeed, recent evidence (Ref 9:445) identifies an excited state of lead oxide (the a state) as obeying case c coupling.

Historically most analyses of lead oxide have used a case c coupling scheme for correlating the molecular energy states with the separated atom states from which they arise. For comparison sake, this will be done here also.

#### Separated Atom - Molecule Correlation

Since lead has a  $6s^2 6p^2$  configuration and oxygen has a  $2s^2 2p^4$  configuration, lead oxide will have six P electrons which constitute a closed shell. Therefore the ground state of lead oxide will be given by  $^1\Sigma^+$ , where the + indicates that the molecular orbitals are symmetric with respect to reflection in the plane of the internuclear axis. In this derivation we consider only the S and P electrons to be involved in transitions. Since lead and oxygen are from different groups in the periodic chart, we must adopt Mulliken's convention for the molecular orbital representation. Following Mulliken (Ref 10:452), we have for the ground state of lead oxide,

$$Z\sigma^2 Y\sigma^2 W\pi^4 X\sigma^2$$

The four most probable excited state molecular orbital configurations and their corresponding spectroscopic states are shown in Table II. This information is shown for both coupling cases. (Ref 2:335)

TABLE II

Molecular Orbitals and Spectroscopic Terms

<u>M.O.</u>	<u>Case a</u>			<u>Case c (<math>\Omega</math> values)</u>
$\pi^3_{\pi}$	$1^+_{\Sigma_0}$	$1^-_{\Sigma_0}$	$1_{\Delta_2}$	$3, 0^+, 0^0, 2, 1$
	$3^+_{\Sigma_{1,0}}$	$3^-_{\Sigma_{1,0}}$	$3_{\Delta_{3,2,1}}$	$1, 0, 0, 2, 1$
$\pi^3_{\sigma}$	$1_{\pi_1}$	$3_{\pi_{i_{2,1,0}}}$		$2, 1, 1, 0^+, 0^-$
$\sigma\sigma$	$1^+_{\Sigma_0}$	$3^+_{\Sigma_{1,0}}$		$1, 0^+, 0^-$
$\sigma\pi$	$1_{\pi_1}$	$3_{\pi_{r_{0,1,2}}}$		$2, 1, 1, 0^+, 0^-$

In Table II the various separated atom states are shown with their corresponding case c  $\Omega$  values. The  $\Omega$  values from the separated atom states must now be correlated

TABLE III

Separated Atom States and  $\Omega$  Values

<u>Pb</u>	<u>0</u>	<u>PbO States (<math>\Omega</math> values)</u>
$3P_0$	+ $3P_2$	$0^+, 0^-, 1, 2$
$3P_0$	+ $3P_1$	$0^+, 0^-, 1$
$3P_0$	+ $3P_0$	$0^+, 0^-$
$3P_1$	+ $3P_2$	$0^+, 0^-, 1, 1, 2, 2, 3$
$3P_1$	+ $3P_1$	$0^+, 0^-, 1, 1, 2$
$3P_1$	+ $3P_0$	$0^+, 0^-, 1$

with the  $\Omega$  values arising from the molecular orbital configurations and the spectroscopic states in Table III. This correlation is shown in Figure 4. The ordering of the spectroscopic states, the designations of the observed (lettered) states, and the  $\Omega$  correlation to separated atoms are based on Oldenberg, Dickson, and Zare, (Ref 4), and Barrow, Fry, and LeBargy (Ref 9). In Figure 4 the energies of the states are not to scale, and the relative positions of some of the unobserved states still need to be verified. The selection rules for case c coupling are,

$$\Delta\Omega = 0, \pm 1, \quad + \leftrightarrow -$$

where + or - indicates that the molecular orbitals are symmetric or anti-symmetric, respectively, with respect to reflection through a plane containing the internuclear axis. With these rules we see from Figure 4 that all the observed transitions except  $b0^- - X0^+$  correspond to allowed transitions. In the  $b0^- - X0^+$  transition the reflection symmetry selection rule is violated, and the transition is dipole forbidden. If the b state obeyed strict case a coupling it would probably never be observed experimentally. In case c coupling, however, the  $+ \leftrightarrow -$  selection rule is not as stringent as in case a. (Ref 2) The fact that the b state is observed indicates its case c character.

### Spectra

The emission spectra that are observed from electronically excited diatomic molecules can be most easily explained by the use of a potential energy curve. Two such curves are shown in Figure 5. The upper curve represents a molecule in an excited state while the lower curve represents the ground state. The various vibrational states in which the molecule may exist are shown within each potential curve. The vibrational levels in the excited state are labeled with  $V'$  and those in the ground state

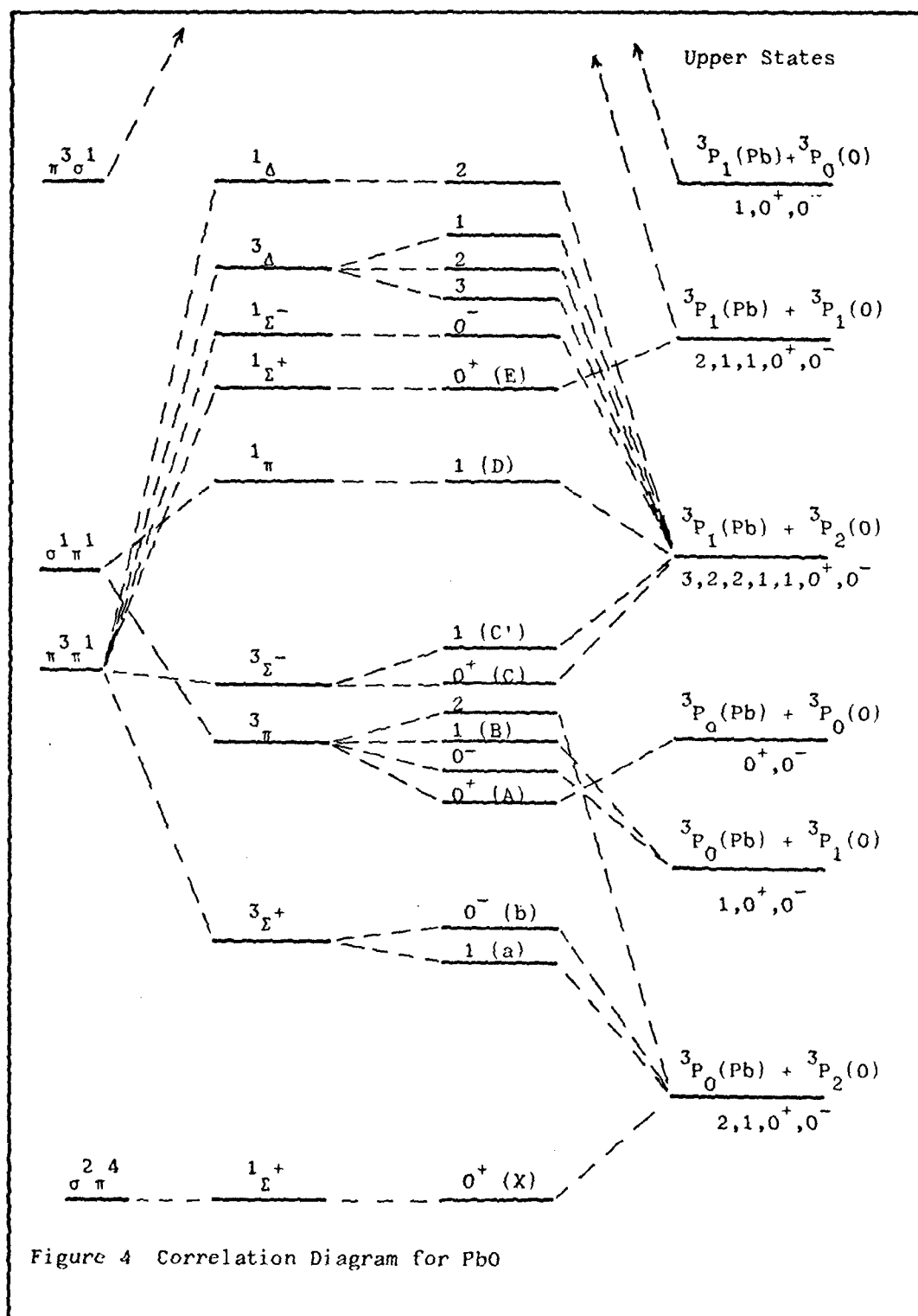


Figure 4 Correlation Diagram for PbO

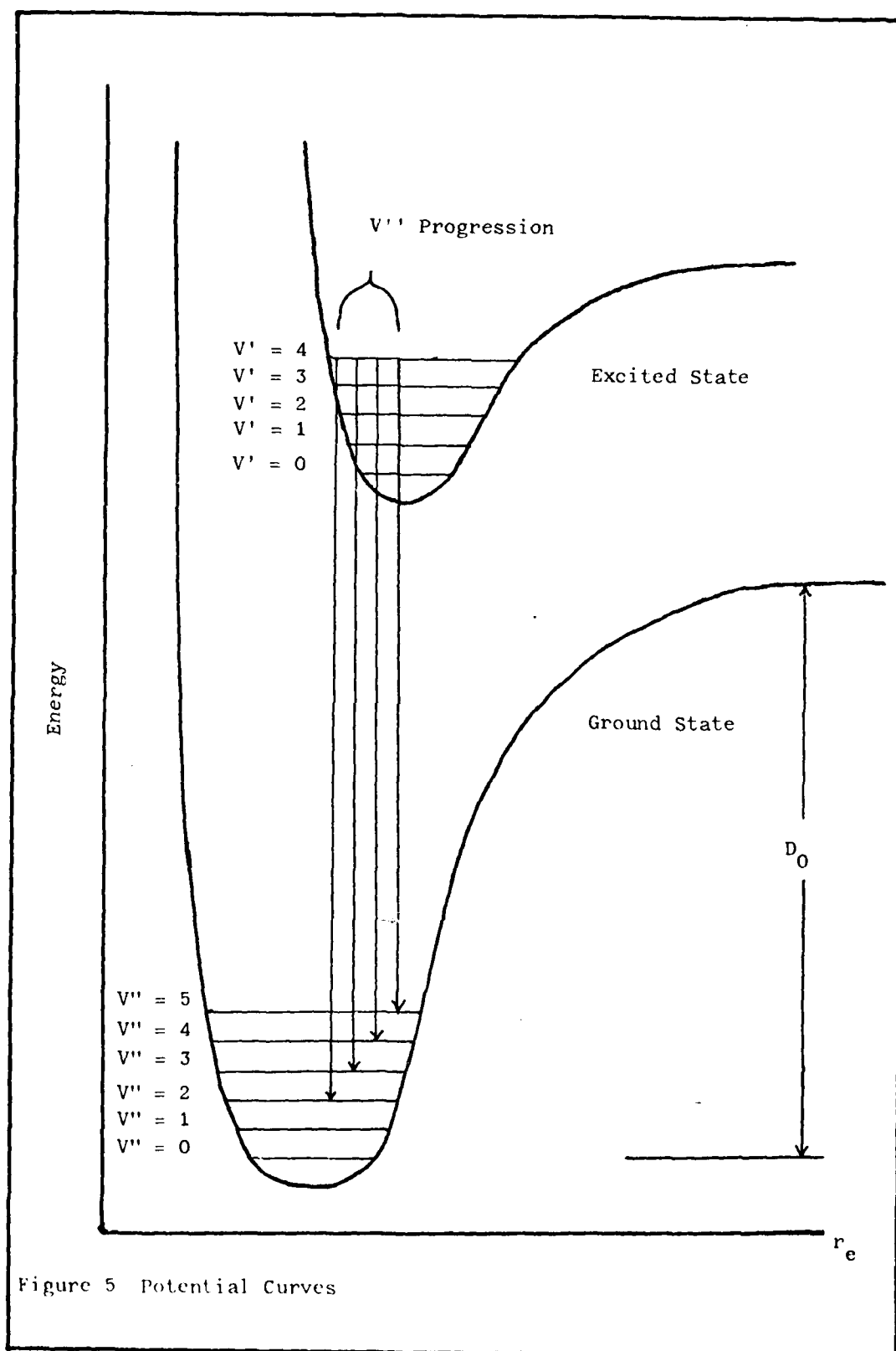


Figure 5 Potential Curves

$V''$ . The vertical axis is energy and the horizontal axis is internuclear distance, denoted by  $r_e$ . Each potential energy curve represents the potential energy well which "binds" the molecule. The energy difference between the  $V=0$  vibrational level and the top of the right side of the well represents how much energy would have to be added to a molecule in the lowest vibrational state to cause the molecule to separate into individual atoms. The energy difference is called the dissociation energy and is designated by  $D_0$ . (See Figure 5.) The spectral bands that are observed correspond to transitions from the various vibrational levels in the excited state down to the various vibrational levels in the ground state. The strength of these various transitions depends on two factors: the population of molecules in the particular excited state vibrational and how closely the internuclear separations of the two states are matched. Clearly, if populations are high in the excited state vibrational levels then this would tend to increase the strength of transitions. To see how internuclear separation affects transition strengths, we make use of the Frank-Condon principle. (Ref 1:120) This principle states that an electron transition can take place much faster than a molecule can vibrate. Therefore, in the time required to make an electronic transition in a diatomic molecule the separation of the two nuclei does not change significantly. Using this result it can be seen quite easily which transitions are likely to have appreciable intensity. Looking at Figure 5, we see that the electronic transitions can now be represented by vertical lines drawn from vibrational levels in the excited state to vibrational levels in the ground state (vertical lines because  $r_e$  does not change). Clearly, if the two electronic states have nearly the same  $r_e$ , then the potential exists for a large number of lines. On the other

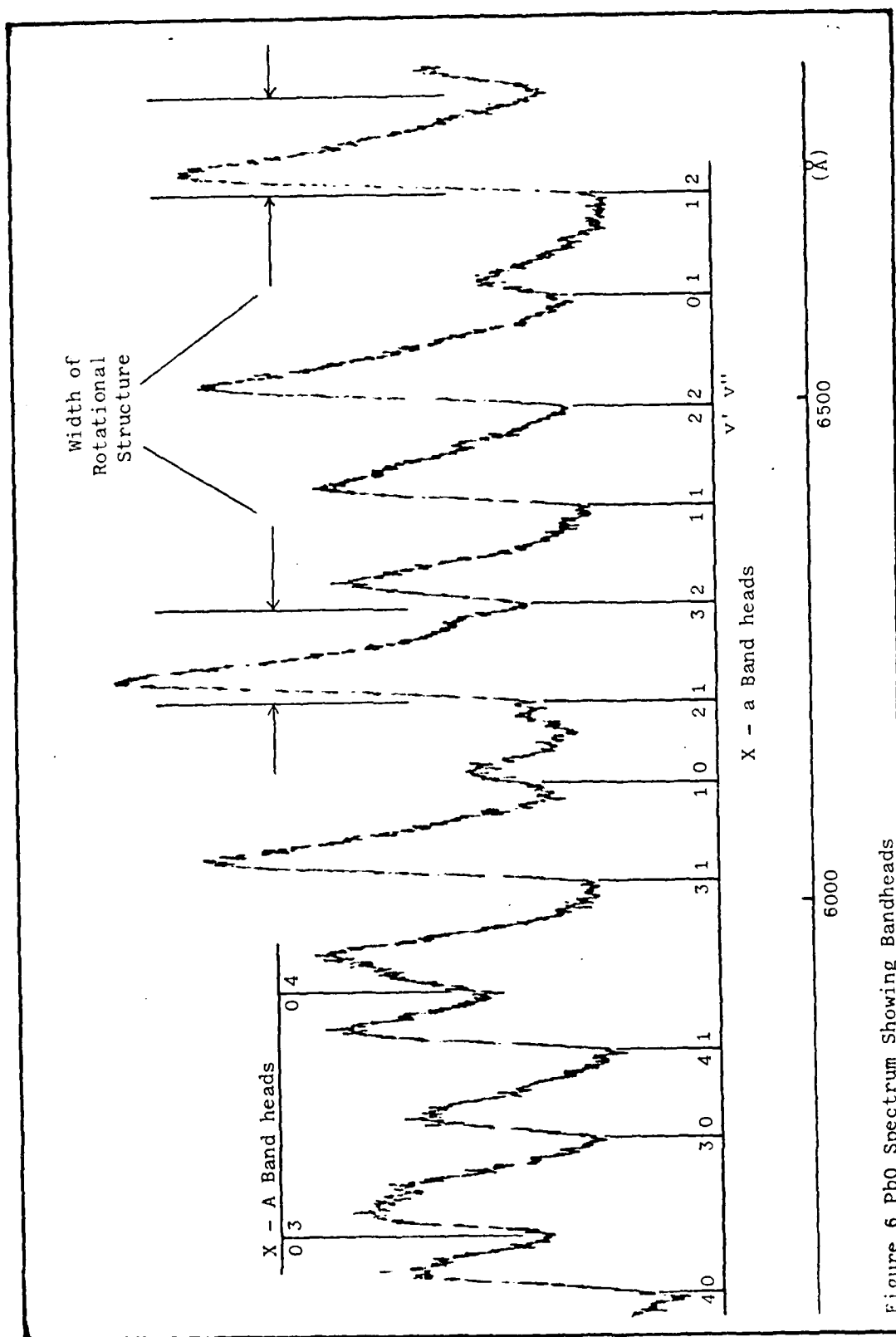


Figure 6 PbO Spectrum Showing Bandheads



hand, if the two states have widely differing  $r_e$  values, then very few lines will be observed. A common feature of spectra such as this is the progression. A progression may occur in two ways. First, transitions may occur from a series of  $V'$  states to be same  $V''$  state. This is called a  $V'$  progression. Alternately, transitions can also occur from a single  $V'$  state to a series of  $V''$  states. This is called a  $V''$  progression. The energy separation of the lines observed in a progression will correspond to the energy difference in the vibrational levels of the appropriate state.

Due to the presence of rotational structure, the observed transitions are typically very wide (many tens of  $\text{\AA}$ ). The finer structure of this spectra are only observed under very high resolution. In the rotational structure the lines from the P, Q, and R branches typically become very closely spaced and run together near one side of the band. This results in the band having a very steep edge on one side called a band head. These features are illustrated in Figure 6. In Figure 6 the band heads of the transitions are labeled with their corresponding electronic and vibrational designations.

#### Reaction Exothermicities

The heats of formation,  $\Delta H_F$ , of various forms of lead, lead oxide, and oxidizers are shown in Table IV. (Ref 13, 14)

TABLE IV

#### Heats of Formation

<u>SUBSTANCE*</u>	<u><math>\Delta H_F</math> (kcal/mol)</u>
Pb(g)	+46.34
PbO(g)	+11.48
O <sub>2</sub>	0
N <sub>2</sub> O	+19.49
O	+59.56

\*(g) = gaseous

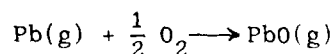
From these heats of formation the exothermicities of various lead-oxidizer reactions can be calculated. These are shown in Table V. A comparison

TABLE V

Reactions and Exothermicities

<u>REACTION</u>	<u>EXOTHERMICITY (cm<sup>-1</sup>)</u>
1) $\text{Pb(g)} + \text{O} \longrightarrow \text{PbO(g)}$	33,051.5
2) $\text{Pb(g)} + \text{O}_3 \longrightarrow \text{Pb(g)} + \text{O}_2$	24,089.7
3) $\text{Pb(g)} + \text{N}_2\text{O} \longrightarrow \text{PbO(g)} + \text{N}_2$	19,013.6
4) $\text{Pb(g)} + \text{O}_2 \longrightarrow \text{PbO(g)} + \text{O}$	
$\text{Pb(g)} + \text{O} \longrightarrow \text{PbO(g)}$	24,390.5

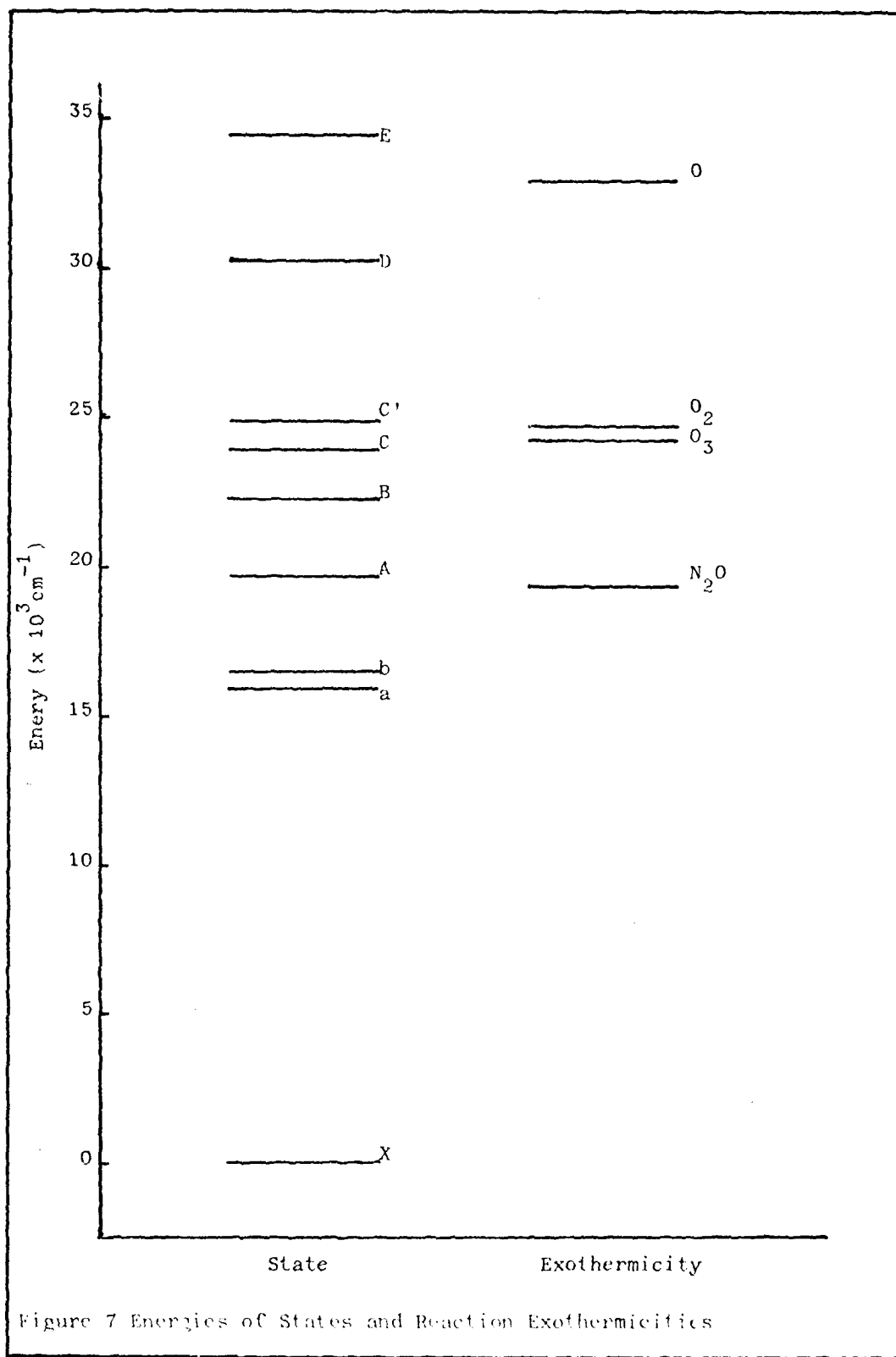
of the reaction exothermicity with various electronic states gives a rough indication of what excited electronic states the particular reactions are likely to populate. Figure 7 shows such a comparison. The chemistry of the  $\text{O}_2$  reaction is reportedly complex and not well understood. (Ref 3:401) Reaction (4) in Table V is just one possible route the reaction may take. Indeed, Linton and Broida (Ref 3:401) found that the reaction,



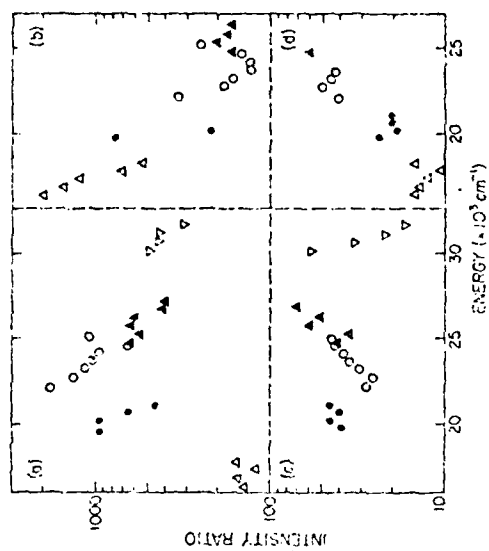
was probably not primarily responsible for the emission studied with  $\text{O}_2$  as the oxidizer. It should be pointed out the values given for the reaction exothermicities are a macroscopic average of the energy which is actually released in each individual atomic event. For this reason, electronic states which lie somewhat higher in energy than a certain exothermicity may still be populated by that same reaction.

Background

The  $\text{PbO}$  molecule has been extensively investigated. Bloomenthal (Ref 8) did early high resolution work by using a uranium lead arc in air



to excite the emission. The work positively identified lead oxide as the emitting species by observing isotopic shift in the spectra due to the presence of three different lead isotopes. Bloomenthal was proceeded in his work by Eder and Valenta, who observed lead oxide emission by introducing lead dichloride into an oxygen gas flame, and Grebe and Konen, who introduced both uranium and ordinary lead dichloride into a carbon arc in air. (Ref 8:34) In both cases the emission observed was tentatively identified as lead oxide, but this was not confirmed until Bloomenthal's work. High resolution absorption studies of lead oxide have been carried out by a number of researchers, including: Shawhan and Morgan (1935), Howell (1935), Vago and Barrow (1947), and Barrow, Deutsch, and Travis (1961). (Ref 4:284) Shawhan and Morgan first identified the E system. All of these absorption studies lead to improved values for the vibrational and rotational parameters. In 1975, there were two reports on the observation of lead oxide emission from the  $Pb + O_3$  chemiluminescence reaction. Oldenborg, Dickson, and Zarc (Ref 4) primarily observed emission from the a and b states. They also used a pulsed laser to make several lifetime measurements of excited states. Kurylo and his associates (Ref 5) were able to observe the b state extensively. No research, other than that by Linton and Broida (Ref 3), has been reported on the change in spectra due to variations in oxidizer pressure in chemiluminescent flames. Linton and Broida studied reactions with different oxidizers and excited gases. In order to make a comparison of spectral behavior in the presence of different oxidizers and excited gases at different pressures Linton and Broida presented data in the following manner. With all other experimental conditions identical, the ratio of the intensity of spectral lines at two different oxidizer pressures was



Graphs of intensity ratio against upper state energy for  $\text{PbO}$  band systems. (a)  $\text{Pb} + \text{O}_2$ ; ratio  $= I(0.4 \text{ Torr})/I(0.2 \text{ Torr})$ ; (b)  $\text{Pb} + \text{N}_2\text{O}$ ; ratio  $= I(3.4 \text{ Torr})/I(3.4 \text{ Torr})$ ; (c)  $\text{Pb} + \text{O}$ ; ratio  $= I(0.5 \text{ Torr})/I(1.7 \text{ Torr})$ ; (d)  $\text{Pb} + \text{N}_2\text{O}$  at 7.5 Torr; ratio  $= I(\text{with active nitrogen})/I(\text{without active nitrogen})$ . The intensity ratio scale is absolute only in graph d. Uncertainties in the ratios are around 30%.

Legend:  $\Delta$ , a-X;  $\bullet$ , A-X;  $\circ$ , B-X;  $\blacktriangle$ , C-X;  $\nabla$ , D-X.

Figure 8 Intensity Ratio Plots (Linton and Broida's results)

plotted as a function of the energy of lines above the ground state. Figure 8 is taken directly from Linton and Broida's work (Ref 3), and shows their results. The semi-log nature of the graph allows population level comparisons to be made more easily between the experimental data and the theoretically predicted exponential behavior (Boltzmann distribution). As seen in Figure 8b for the  $\text{Pb} + \text{N}_2\text{O}$  reaction, as the oxidizer pressure was varied from 3.4 to 34 Torr the most intense emission shifted from shorter to longer wavelengths (blue to red), that is, emission from the a state was increased relative to the A and B states. As Linton and Broida point out, for the a state the downward linear trend of the data points (presumable a  $V'$  progression with  $V'' = 0$ ) indicates that as the pressure is increased there is a decrease in the vibrational temperature and that the vibrational populations can be closely described by an Boltzmann distribution. Data for the other states does not exhibit a linear trend. Also, a linear trend in the populations of the electronic states is not as apparent as it is in the vibrational levels of the a state. No data is available on pressure variation with just  $\text{O}_2$  as the oxidizer. Linton and Broida could not obtain data here because of severe system fouling problems encountered in the  $\text{Pb} + \text{O}_2$  reaction.

### III. Experimental Apparatus

#### Introduction

In this chapter the experimental equipment used in this research will be described. A brief description of the flow tube reactor will be given. A detailed discussion is given in Reference 15 and will not be repeated here. Modifications which were made to the flow tube apparatus for this experiment will be discussed in detail.

#### Set-Up

The experimental set-up used for these experiments is shown in Figure 9. A gas flow tube reactor was used to generate the chemiluminescent reactions (Ref 15). The flow tube was constructed of three inch inner diameter stainless steel tube made by Alloy Products. Sections were fastened together with quick flanges. O-rings between the sections insured vacuum tight seals. The flow tube was characterized by laminar flow. (Ref 15:47) Dynamic pressures in the flow tube were measured downstream from the reaction region with an MKS Baratron 77 pressure meter. A furnace assembly, attached to the flow tube body beneath the reaction region, was used to generate the lead vapor. The lead vapor was generated by resistively heating reagent grade granulated lead (Baker Analyzed, 99.7% pure) in an aluminum oxide ceramic crucible (R. D. Mathis Company). The heating coil was of tungsten wire (R. D. Mathis Company) wound around the crucible and connected to electrodes at each end; see Figure 10. Argon gas was introduced into the furnace chamber to carry the lead vapor out of the furnace chamber and into the reaction region. The argon vapor also served to cool the lead vapor before it reached the reaction region. This cooling reduced the thermal excitation of the lead which reduced the probability of observing atomic emission lines. (Ref 6:164) In the

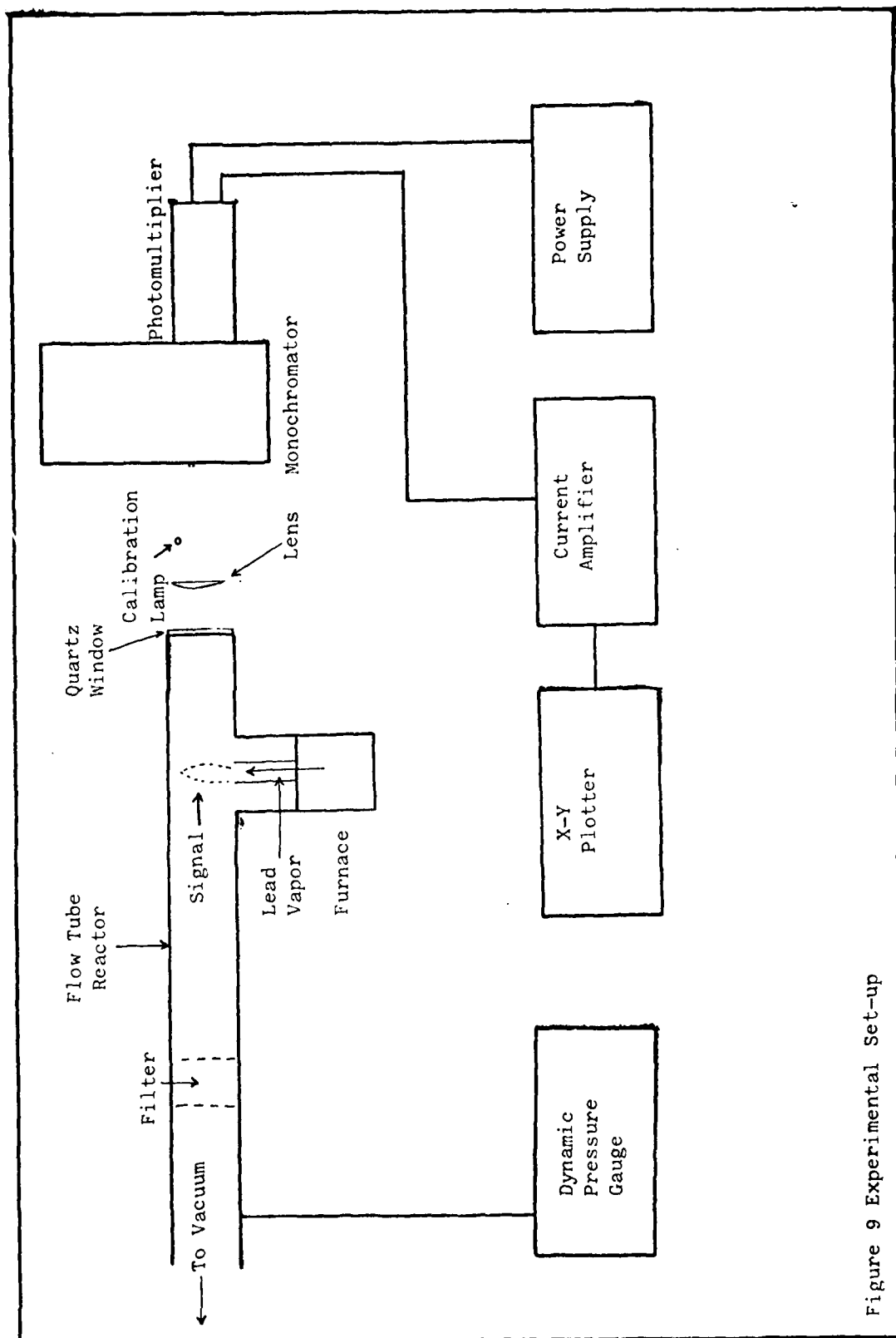
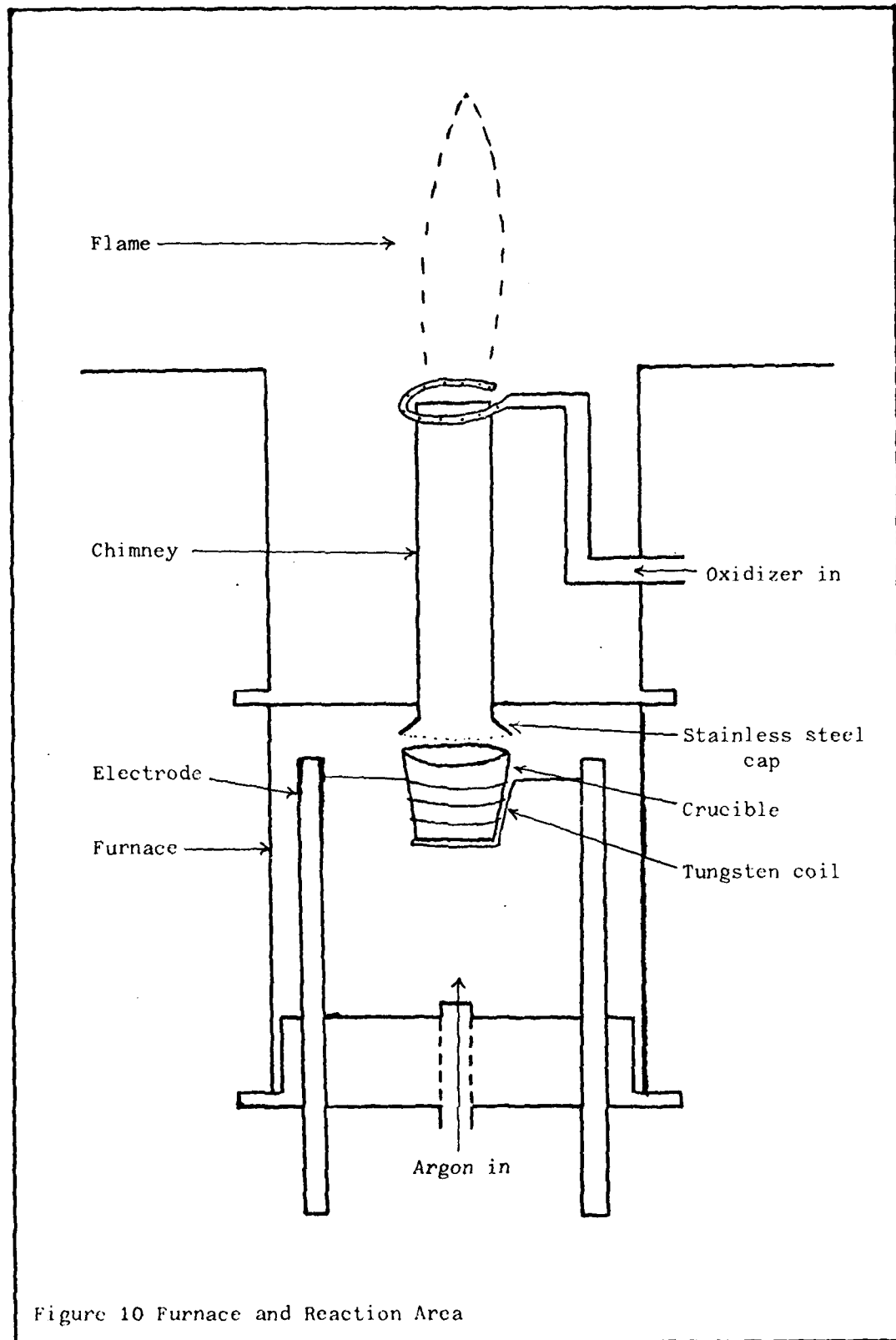


Figure 9 Experimental Set-up





reaction region this lead-argon mixture met the oxidizer and a chemiluminescent flame resulted. A quartz window was located 26.5 cm upstream of the chemiluminescent flame. A 5.6 cm clear diameter planar-convex lens with an 8.0 cm focal length was positioned 6.8 cm from the quartz window. The lens focused the signal onto the entrance slit of the monochromator 12.0 cm away. The monochromator was a Jarrell-Ash .25 m with an Ebert optical mount. Grating response curves are shown in Appendix A. Motor drives allowing scan speeds of 50, 100, 150, 200, 250, and 400 A per minute were available. It was experimentally determined that when working at 5000 Å in first order, using 150 μm slits, and operating at a scan speed of 200 A per minute, the monochromator was roughly capable of resolving peaks 9 Å wide (FWHM) and 12 Å apart with a dip between the peaks to approximately the half-intensity point. Oriel pen-ray lamps were used for calibration. Mounted on the exit slit of the monochromator was an RCA 7265 photomultiplier tube sensitive in the range 3000 - 8000 Å. The photomultiplier was biased with a Keithley Model 244 high voltage supply. Photomultiplier data is shown in Appendix B. A Keithley Model 427 current amplifier was used to amplify the signal from the photomultiplier tube. This amplified signal was then used to drive a Houston Instrument, Series 2000, Omnigraphic X - Y recorder. The recorder produced a plot of signal intensity versus wavelength.

#### Flow Tube Modifications

Prior to the start of these experiments, the top of the furnace chamber was configured as shown in Koym's thesis. (Ref 15:38) Previous runs made with this configuration resulted in large lead deposits in the furnace and weak flames. (Ref 15:66) For these reasons a stainless steel cap was silver soldered to the base of the chimney. (See Figure 10.)

The cap is slightly wider than the crucible top and approximately 0.3 - 0.6 cm above the crucible lip. This modification resulted in improved throughput of lead vapor into the reaction region and hence a more intense chemiluminescent flame.

A second problem encountered previously with this apparatus was severe coating of the observation windows by the reaction products to the extent that often not even a single spectra could be taken. (Ref 15:66) When the pathlength from flame to window was very short ( $\sim 8$  cm), the coating was severe and very rapid. A number of things were done in an attempt to alleviate this problem. First, in reference 15, observations were made perpendicular to the flow tube axis. The set-up was changed so that observations could be made from upstream of the flame. Secondly, a gas curtain, based upon the recommendation in reference 15, was fashioned. (See Figure 11.) This gas curtain was just a means of introducing an inert gas between the window and the flame upstream of the flame.

The curtain was designed to minimize the amount of reaction products which could make their way upstream to the observation window. One further modification was the positioning of an aluminum slit assembly between the flame and the curtain. The slit was wide enough not to obscure the flame as viewed by the lens. As before, this configuration was designed to restrict the flow of reaction products toward the window.

Both the gas curtain and slit assembly failed to reduce the severity of the coating problem. Argon and helium gases were introduced into the curtain at various pressures from 0.05 to 10 Torr. At no point was the coating rate visibly diminished. Viewing the flame from upstream and lengthening the distance from the flame to window reduced the coating rate to an acceptable level.

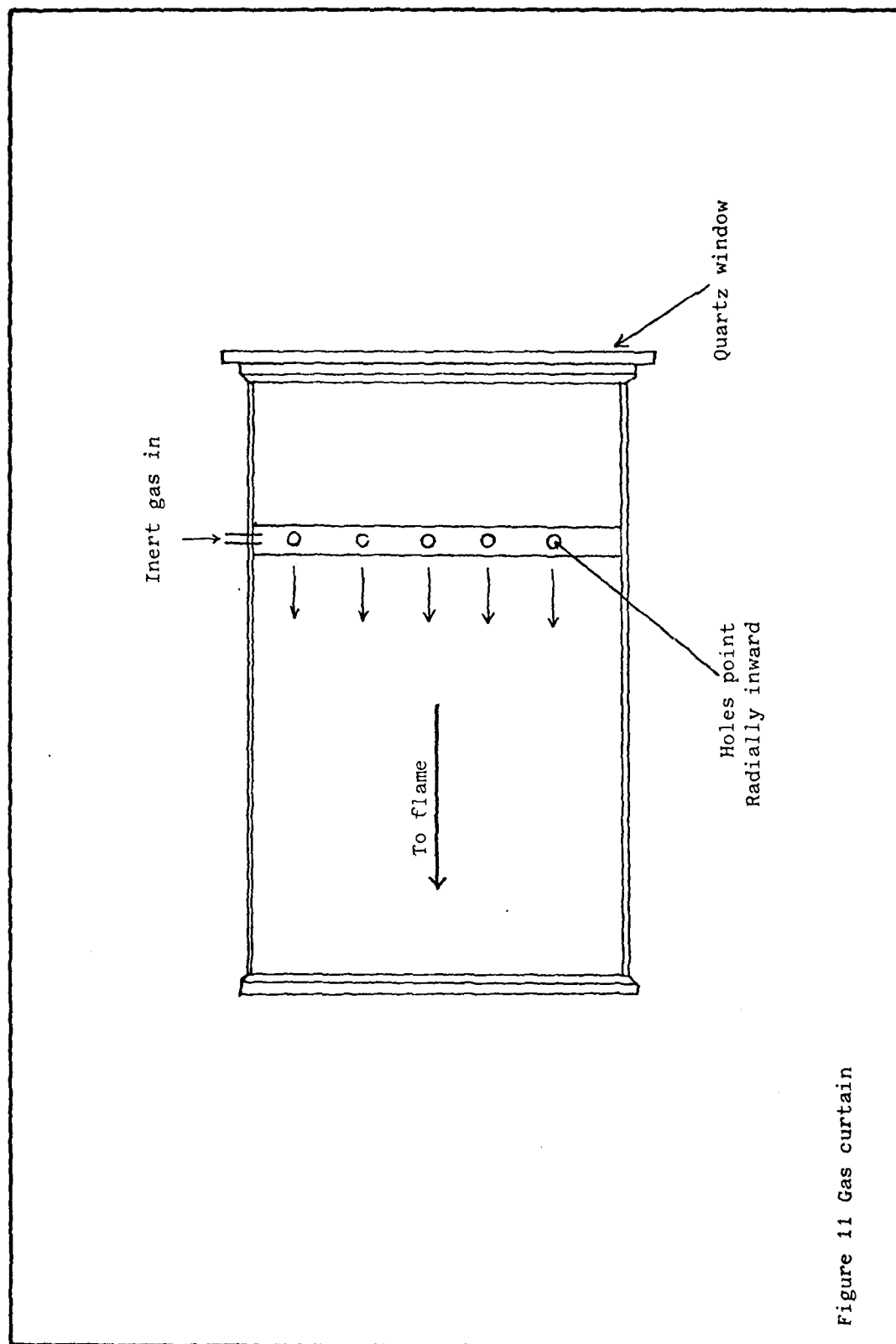


Figure 11 Gas curtain

#### IV. Experimental Procedure

##### Introduction

The start-up and shut down procedures for the flow tube reactor are given in reference 15. Here, only operational procedures of experimental interest will be mentioned. The procedures used in system alignment, spectrum calibration, and electrical noise reduction will be discussed in detail.

##### General Procedures

The vacuum pumps used in this experiment was semi-rigidly coupled to the flow tube and, if allowed to do so, would generate unacceptable levels of vibration throughout the system. Attempts at alignment under these conditions were marginal at best. For this reason, approximately 200 pounds of lead weights were loaded onto each pump to damp vibrations. This technique proved quite adequate in eliminating all but the smallest of vibrations.

Prior to making each run the quartz window was cleaned of deposits. The cleaning was accomplished with a laboratory liquid soap, Micro, and water. In addition, the window was cleaned with the application of collodion. The dried collodion film was peeled off along with any last remaining traces of deposit.

Lead deposits were removed from the base of the chimney prior to each run. Failure to do this would result in an increasingly smaller chimney aperture at the base which restricted lead vapor throughput.

Regularly, after eight or nine runs, the tube was disassembled and cleaned of loose by-products. This is not a stringent requirement, but it does diminish the severity of the window coating because there are fewer reaction products being circulated in the tube. Whenever the flow

tube was disassembled the filter (glass wool; located between flame and pumps) was changed. This maintained the maximum throughput in the flow tube body.

Lead is an inhalent hazard. (Ref 16) The following measures were taken to minimize this danger. If it became necessary to repair a part of the tube or handle it extensively, the part was washed in soap and water and then rinsed in strong solvents, methylene chloride and acetone. All cleaning operations were done inside a negative pressure hood assembly. The tube was not opened until the reaction products had condensed out. The amount of products still suspended in the tube could be crudely determined by observing the amount of scattered radiation from a helium-neon laser beam directed into the tube.

Each time the flow tube was operated it was first evacuated to approximately 120 um of mercury pressure before other gases were introduced. Lead vapor densities in the tube during operation were on the order of  $10^{14}$  atoms/cm<sup>3</sup>.

#### Alignment

The lens-monochromator-photomultiplier system was aligned in the following manner. A xenon calibration lamp (Oriel, Pen-ray) was inserted through the chimney into the position of the flame. The tall, narrow shape of the lamps glow approximated the shape of the flame. The lamp was oriented so that its emission would pass through the quartz observation window. The focusing lens was then centered horizontally in front of the window but positioned slightly above center vertically. The slight off-centering insured that the background glow from inside the chimney would not be focused into the monochromator (This background glow was from the hot tungsten heating coil and peaked around 7300 A.)

The exact desired vertical position of the lens was most easily determined by observing the image of the lamp on the entrance slit of the monochromator. When the lens position was approximately correct, the monochromator was positioned so that the image of the lamp fell directly on the entrance slit and was centered vertically on the slit. With the monochromator adjusted to be level, small horizontal adjustments were made to bring the exit slit into proper alignment. Since the photomultiplier tube was rigidly mounted to the exit slit no further alignment was necessary.

#### Calibration

Spectra were calibrated during the analyses of the flame by placing a small calibration lamp near the optical axis between the focusing lens and the monochromator. (See Figure 9.) When the wavelength indicator on the monochromator approached a calibration peak the lamp was switched on momentarily. The flame signal was covered during calibration to insure that the spectra were not distorting the calibration lines. The small off-axis position of the calibration lamp had no detectable effect on the position of the calibration peaks. Xenon, neon, and mercury lamps were all used. Two calibration lines placed on each spectra were used to calculate an  $\text{\AA}/\text{cm}$  figure for each plotted spectra. One of the lines was then chosen as a reference and a wavelength calculated for all the lines based on how far away the lines were from the reference. In some cases where strong band heads had been identified previously, calculated wavelength values of these band heads were used to calibrate the spectra internally.

#### Noise Reduction

A search was made of the operating regimes of the photomultiplier

tube and current amplifier to determine what settings provided the best signal to noise ratio. The procedure is described. With no signal present the X-Y plotter was zeroed with the plotter zero adjust knob and the current amplifier fine adjustment. The zero positions from the two adjustments were to coincide. The monochromator was then dialed to a strong calibration line. The lamp was adjusted to yield about a two-thirds scale deflection on the plotter. The noise level and deflection at this point were then compared to other settings of photomultiplier voltage and current amplification after going through the same procedure for each setting.

It was also noted that a further reduction in electronic noise could be achieved by grounding the metallic case of the monochromator and wrapping all coaxial connectors with non-conducting tape and aluminum foil.

A small further reduction in noise was also achieved when the current amplifier and high voltage supply were grounded separately from all other equipment.



## V. Results and Discussion

This section is presented in three parts. In the first section some general remarks on the flow tube performance and characteristics are given. In the next section assignments of all spectral lines are made and compared to theoretical values. Finally, the results of the oxidizer experiments are presented. Appendix C is a compilation of representative spectra which were taken during the course of the experiments.

### Flow Tube Performance and Experimental Observations

During the course of these experiments a number of different reaction products were observed in the flow tube following shutdown. The predominant feature of the  $\text{Pb} + \text{N}_2\text{O}$  reaction was a black powdery residue ( $\text{Pb}_2\text{O}$ ) which coated the inside of the flow tube and the observation window. Smaller amounts of a yellow powder ( $\text{PbO}$ ) and a gray powder ( $\text{Pb}$ ) were also present. During some runs, however, no black residue was present and the only coating on the observation window was a faint blue film. This blue film remains unidentified.

In the  $\text{Pb} + \text{O}_2$  reaction absolutely no black powder ( $\text{Pb}_2\text{O}$ ) or blue film were produced. This result is in direct disagreement with Linton and Broida (Ref 3:401) who reported rapid system fouling with  $\text{Pb}_2\text{O}$  in the  $\text{Pb} + \text{O}_2$  reaction. In this experiment, the primary reaction product generated in the  $\text{Pb} + \text{O}_2$  reaction was  $\text{PbO}$ . Large quantities of this bright yellow powder thoroughly coated the inside of the flow tube. On the top of the flow tube, immediately above the chimney and the flame, a deposit of bright red powder ( $\text{Pb}_3\text{O}_4$ ) also built up. This deposit was observed to grow downward toward the chimney with time. Generally, window coating was much less severe in the  $\text{O}_2$  reaction than in the  $\text{N}_2\text{O}$  reaction. The scan time of a spectrum was thirteen minutes and generally

while observing the  $\text{Pb} + \text{N}_2\text{O}$  reaction only two or three useful spectra could be taken before window coating forced shut down. In the  $\text{Pb} + \text{O}_2$  reaction, however, the number of spectra which could be taken was limited only by the time it took to evaporate all the lead from the crucible; about three to four hours.

Lower pressures of carrier gas were required in the  $\text{O}_2$  reaction to produce the same intensity flame which required a higher carrier gas pressure in the  $\text{N}_2\text{O}$  reaction. This implies that  $\text{O}_2$  is more efficient at reacting with lead vapor than is  $\text{N}_2\text{O}$ .

Under typical operating conditions (2-6 Torr argon, 0.1 - 0.3 Torr oxidizer) the chemiluminescent flames observed were tall and narrow. At the base the flames were approximately the width of the chimney opening, about 5/8 inch. Under conditions of lower carrier gas pressure (2-4 Torr) the flames would taper gradually to a point in the upper half of the flow tube. Carrier gas pressures above 4 Torr caused the flame to appear as a slightly tapered column the entire height of the tube, about 3 inches. Carrier gas pressures above 7 Torr caused the flame to become broad and diffuse, with a large amount of flicker. It was difficult to obtain any useful spectra under these conditions. Oxidizer pressures above .8 Torr had a similar effect, that is, the flame became very short and flared into several different arms. Again, a large amount of flame flicker was present.

#### Spectra and Assignments

When the flame was sufficiently intense spectra were taken using 150  $\mu\text{m}$  slits. The majority of the spectra were taken using 500  $\mu\text{m}$  slits. Whenever possible, assignments were based on spectra obtained using the narrowest slits and slowest scan speeds. Spectra were observed in the

region 3500 - 9000 Å. Figure 12 and 13 show the spectra of the Pb + N<sub>2</sub>O<sup>o</sup> and Pb + O<sub>2</sub> reactions, respectively, between 3800 and 9000 Å. The band-heads observed during the reaction Pb + N<sub>2</sub>O are listed in Table VI. In addition, values calculated from the spectral parameters ( $\omega_e$  and  $X_e$ ) reported in the literature are listed in the Table with the difference between the two values. The assignments of the bands are shown.

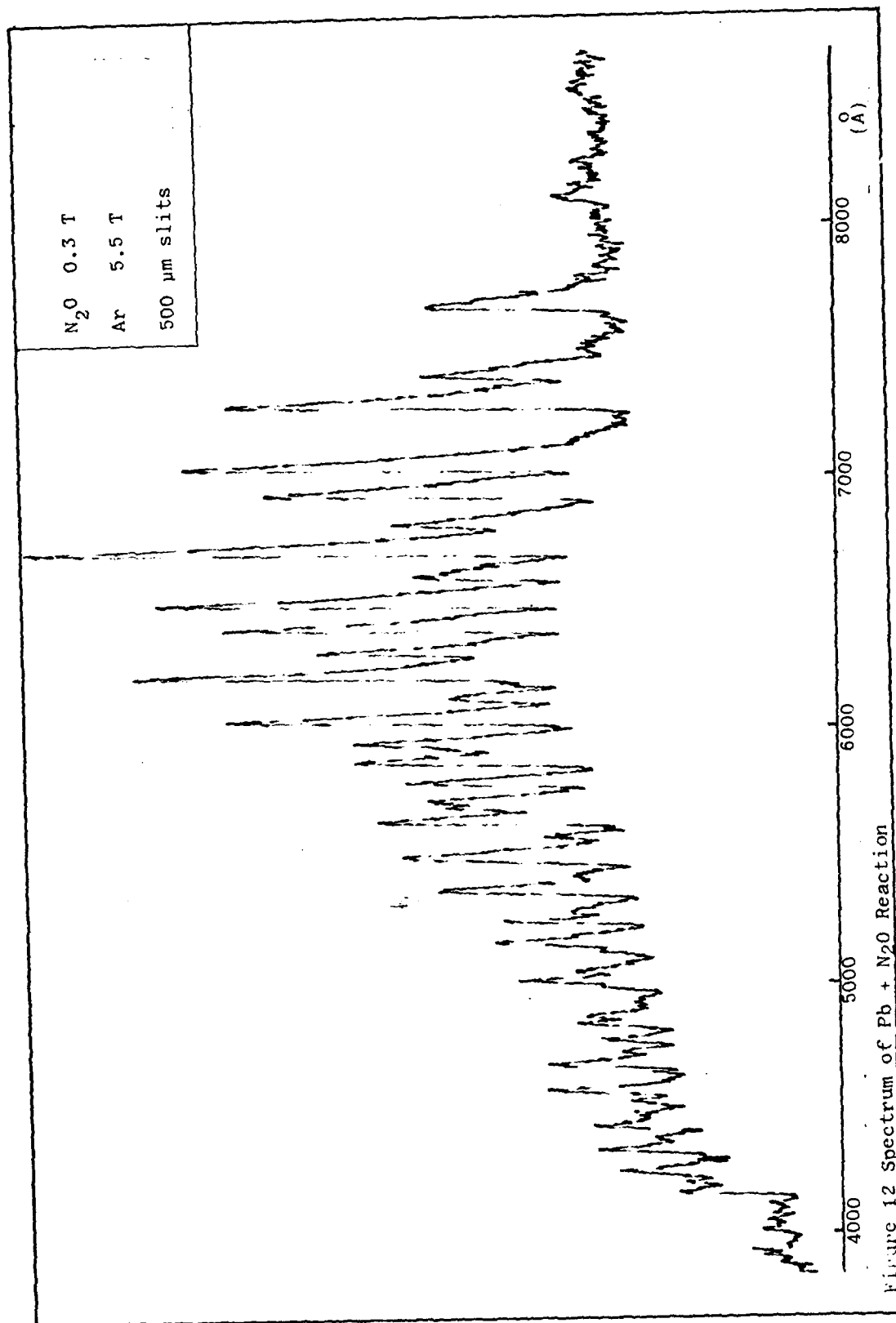


Figure 12 Spectrum of Pb +  $N_2O$  Reaction

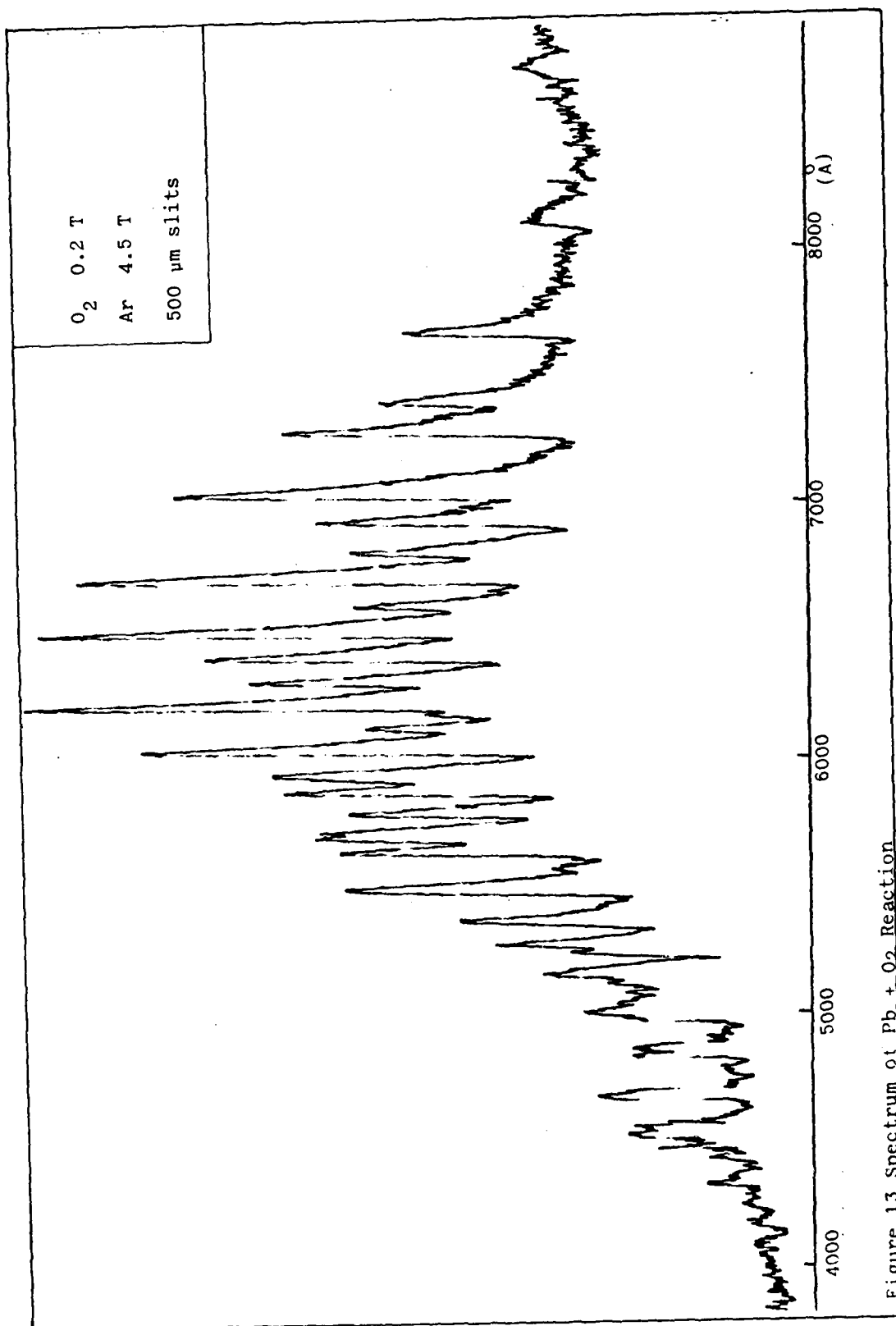


Figure 13 Spectrum of Pb + O<sub>2</sub> Reaction

Table VI

Band heads of the Pb + N<sub>2</sub>O Reaction

<u>OBS.</u>	<u>Wavelengths (Å)</u>		<u>Assignments</u>	
	<u>CALC.</u>	<u>OBS-CALC.</u>	<u>V',V''</u>	<u>TRANSITION</u>
4555.6	4556.2	-0.6	1,1	B-X
4660.1	4660.0	0.1	0,1	B-X
4819.5	4818.8	0.7	0,2	B
4865.6	4868.4	-2.8	1,3	B
4967.3	4965.4	1.9	3,5	B
4991.6	4987.1	4.5	0,3	B
5037.1	5038.4	-1.3	1,4	B
4714.1	4713.2	0.9	5,1	A
4752.6	4750.3	2.3	3,0	A
4835.2	4834.2	1.0	7,3	A
4854.3	4852.0	2.3	2,0	A
4978.9	4982.5	-3.6	4,2	A
5023.7	5026.2	-2.5	2,1	A
5114.7	5113.7	1.0	6,4	A
5140.2	5140.5	-0.3	1,1	A
5262.8	5260.4	2.4	0,1	A
5275.0	5282.8	-7.8	3,3	A
5335.1	5334.5	0.6	1,2	A
5466.0	5463.7	2.3	0,2	A
5497.1	5497.6	-0.5	6,6	A
5682.4	5681.0	1.4	0,3	A
5914.7	5913.9	0.8	0,4	A
5999.9	6000.0	-0.1	1,5	A
6168.7	6164.1	4.6	0,5	A
6252.8	6255.0	-2.2	1,6	A
7149.2	7146.3	2.9	1,9	A
7496.8	7494.8	2.0	1,10	A
4902.0	4889.8	2.2	10,0	a
4994.5	4995.3	-0.8	9,0	a
5105.4	5107.0	-1.6	8,0	a
5229.8	5225.0	4.8	7,0	a
5562.5	5562.5	0.0	6,1	a
5623.5	5623.5	0.0	4,0	a
5775.6	5773.5	2.1	3,0	a
5855.6	5858.7	-3.1	4,1	a
5933.8	5933.4	0.4	2,0	a
6020.7	6021.7	-1.0	3,1	a
6105.1	6104.2	0.9	1,0	a
6199.8	6195.8	4.0	2,1	a
6290.6	6289.4	1.2	3,2	a
6384.7	6382.4	2.3	1,1	a
6479.6	6479.6	0.0	2,2	a

Table VI (cont'd)

<u>Wavelengths (A)</u>			<u>Assignments</u>	
<u>OBS.</u>	<u>CALC.</u>	<u>OBS-CALC.</u>	<u>V', V''</u>	<u>TRANSITION</u>
6582.4	6582.6	-0.2	0,1	a
6683.9	6683.9	0.0	1,2	a
6783.6	6787.4	-3.8	2,3	a
6819.3	6825.8	-6.5	1,8	a
6894.2	6893.0	1.2	3,4	a
6906.4	6903.8	2.6	0,2	a
6998.3	7001.0	-2.7	4,5	a
7011.6	7011.9	-0.3	1,3	a
7123.6	7122.2	1.4	2,4	a
7219.3	7224.0	-4.7	6,7	a
7254.3	7254.3	0.0	0,3	a
7369.8	7369.8	0.0	1,4	a
7454.2	7456.8	-2.6	8,9	a
7638.1	7638.1	0.0	0,4	a
5716.5	5714.7	1.8	3,0	b
6806.5	6810.4	-3.9	3,4	b
7050.2	7049.1	1.1	8,8	b
7478.9	7484.8	-5.9	0,4	b

Table VII

Band Head of the Pb + O<sub>2</sub> Reaction

<sup>o</sup> Wavelengths (Å)			Assignments	
OBS.	CALC.	OBS-CALC.	V', V''	TRANSITION
3496.9	3487.1	9.8	0,2	D-X
3516.1	3508.6	7.5	1,3	D-X
3615.8	3617.9	-2.1	2,5	D
3630.8	3639.7	-8.9	3,6	D
3692.3	3687.1	5.2	1,5	D
3731.9	3731.0	0.9	3,7	D
3764.7	3759.8	4.9	0,5	D
3787.7	3781.8	6.1	1,6	D
4144.4	4144.3	0.1	4,0	B
4230.6	4230.0	0.6	3,0	B
4319.2	4319.4	- .2	2,0	B
4415.7	4412.6	3.1	1,0	B
4508.3	4509.9	-1.6	0,0	B
4660.8	4660.0	0.8	0,1	B
4818.1	4818.8	-0.7	0,2	B
4984.8	4987.1	-2.3	0,3	B
5088.7	5088.9	-0.2	2,5	B
5167.5	5165.7	1.8	0,4	B
5325.4	5322.4	3.0	3,7	B
5615.7	5614.6	1.1	1,7	B
5670.1	5670.6	-0.5	2,8	B
4748.3	4750.3	-2.0	3,0	A
4957.5	4958.4	-0.9	1,0	A
5046.3	5048.0	-1.7	5,3	A
5069.7	5069.9	-0.2	0,0	A
5138.4	5140.5	-2.1	1,1	A
5262.8	5260.4	2.4	0,1	A
5334.2	5334.5	-0.3	1,2	A
5465.0	5463.7	1.3	0,2	A
5682.4	5681.0	1.4	0,3	A
5766.0	5762.8	3.2	1,4	A
5913.6	5913.8	-0.2	0,4	A
6161.8	6164.0	-2.2	0,5	A
6527.6	6529.2	-1.6	1,7	A
5226.8	5225.0	1.8	7,0	a
5351.9	5350.0	1.9	6,0	a
5479.7	5482.6	2.9	5,0	a
5562.7	5562.5	0.2	6,1	a
5623.2	5623.5	-0.3	4,0	a
5706.1	5706.0	0.1	5,1	a



Table VII (cont'd)

<sup>o</sup> <u>Wavelengths (A)</u>			<u>Assignments</u>	
<u>OBS.</u>	<u>CALC.</u>	<u>OBS-CALC.</u>	<u>V', V''</u>	<u>TRANSITION</u>
5771.9	5773.5	-1.6	3,0	a
5858.5	5858.7	-0.2	4,1	a
5931.2	5933.4	-2.2	2,0	a
6022.0	6021.7	0.3	3,1	a
6101.6	6104.3	-2.7	1,0	a
6195.8	6195.9	-0.1	2,1	a
6288.9	6289.4	-1.5	3,2	a
6382.9	6382.4	0.5	1,1	a
6384.8	6384.9	-0.1	4,3	a
6478.5	6479.6	-1.1	2,2	a
6582.4	6582.6	-0.2	0,1	a
6683.3	6683.9	-0.6	1,2	a
6786.0	6787.4	-1.4	2,3	a
6903.6	6903.8	-0.2	0,2	a
7010.7	7011.9	-1.2	1,3	a
7253.5	7254.3	-0.8	0,3	a
7371.7	7369.8	1.9	1,4	a
7486.6	7487.9	-1.3	2,5	a
7641.4	7638.1	3.3	0,4	a
7730.5	7731.8	-1.3	4,7	a
7765.5	7762.0	3.5	1,5	a
8014.8	8018.1	-3.3	3,7	a
8062.4	8060.2	2.2	0,5	a
8150.4	8150.5	-0.1	4,8	a
8194.8	8193.6	1.2	1,6	a
8285.6	8285.7	-0.1	5,9	a
8471.3	8469.3	2.0	3,8	a
6222.3	6220.1	2.2	3,2	b
6541.9	6539.3	2.6	9,7	b
7621.3	7624.7	-3.4	1,5	b
8036.3	8041.1	-4.8	1,6	b
8352.7	8346.5	6.2	3,8	b

Table VII lists similar results for the reaction  $\text{Pb} + \text{O}_2$ . In making the assignments, if it happened that there was more than one calculated value which closely corresponded to an observed bandhead, several pieces of additional information were available to assist in making the correct assignment. For the X-A, X-B, and X-D systems a limited number of Frank-Condon factors were available to indicate the theoretical relative intensities of the transitions. (Ref 17) Frank-Condon factors are numerical quantities based on the electron wave functions and the shape of the potential curves. Frank-Condon factors were not available for the X-a or X-b system. Questions concerning assignments in these systems were resolved with the help of references 4 and 5. These contain extensive tabulations of previously observed bands and their relative strengths. Finally, assignments were made which would complete a progression or sequence where the remainder of the progression or sequence had already been assigned unambiguously and the intensity of the band in question was not inconsistent with the other lines in the progression or sequence.

#### Variation of Oxidizer Pressure

For both experiments data are presented in the manner developed by Linton and Broida (Ref 3:399) and outlined briefly in Chapter II.

$\text{Pb} + \text{O}_2$  Experiment. Five spectral determinations were made in the region 3500 - 8700 Å. In all five spectra the argon carrier gas pressure was kept constant at 2.1 Torr. The five oxidizer pressures were 0.04, 0.1, 0.2, 0.4, and 0.7 Torr. The actual plots of the five spectra are shown in Figure 14. From these plots it is apparent that as the  $\text{O}_2$  pressure was increased from 0.04 to 0.2 Torr there was a gradual increase in the emission intensity from the a, A, and B states. At 0.4 Torr, however, there was a dramatic increase in emission from the B and A states

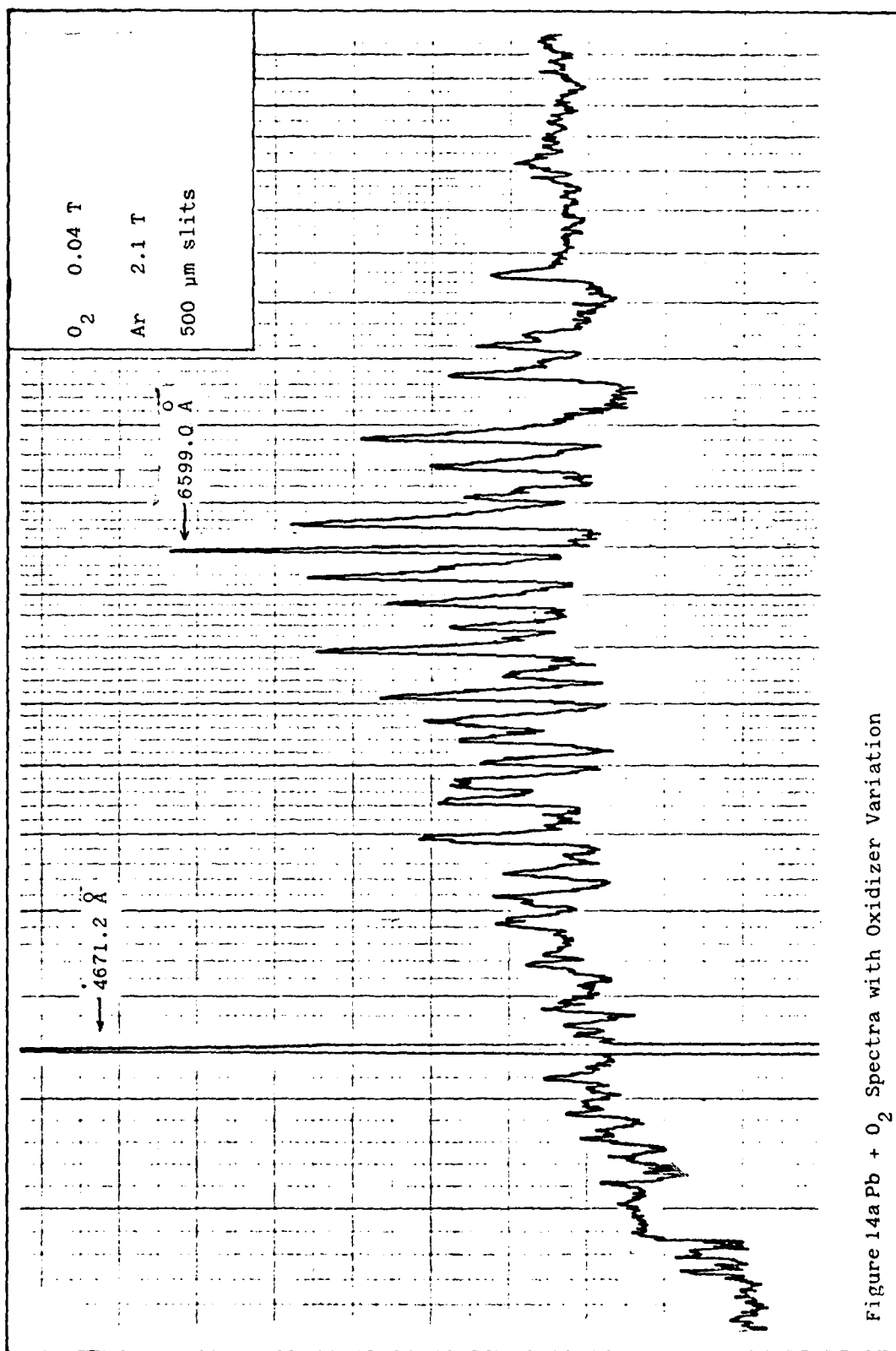


Figure 14aPb +  $O_2$  Spectra with Oxidizer Variation

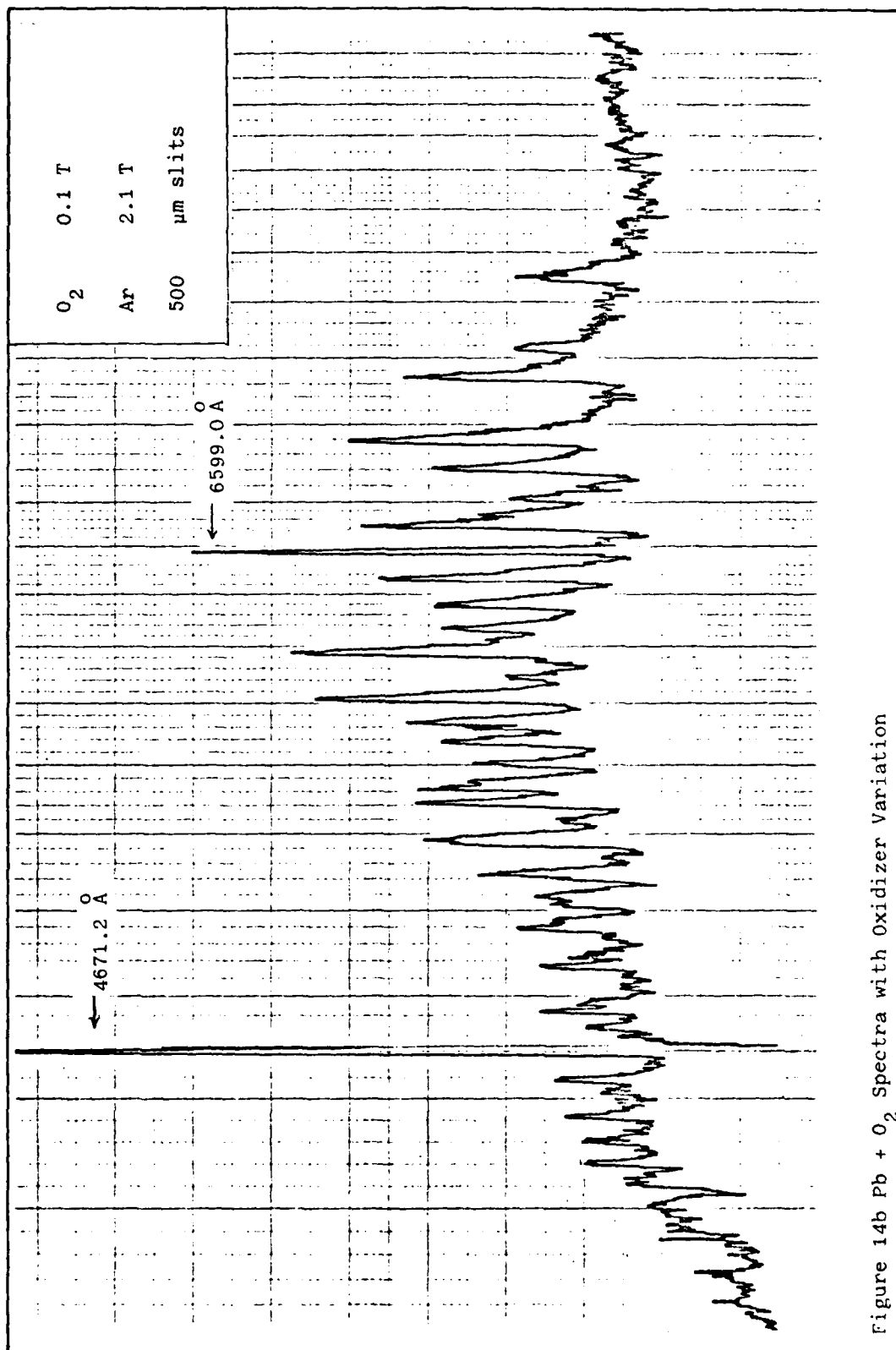


Figure 14b Pb +  $O_2$  Spectra with Oxidizer Variation

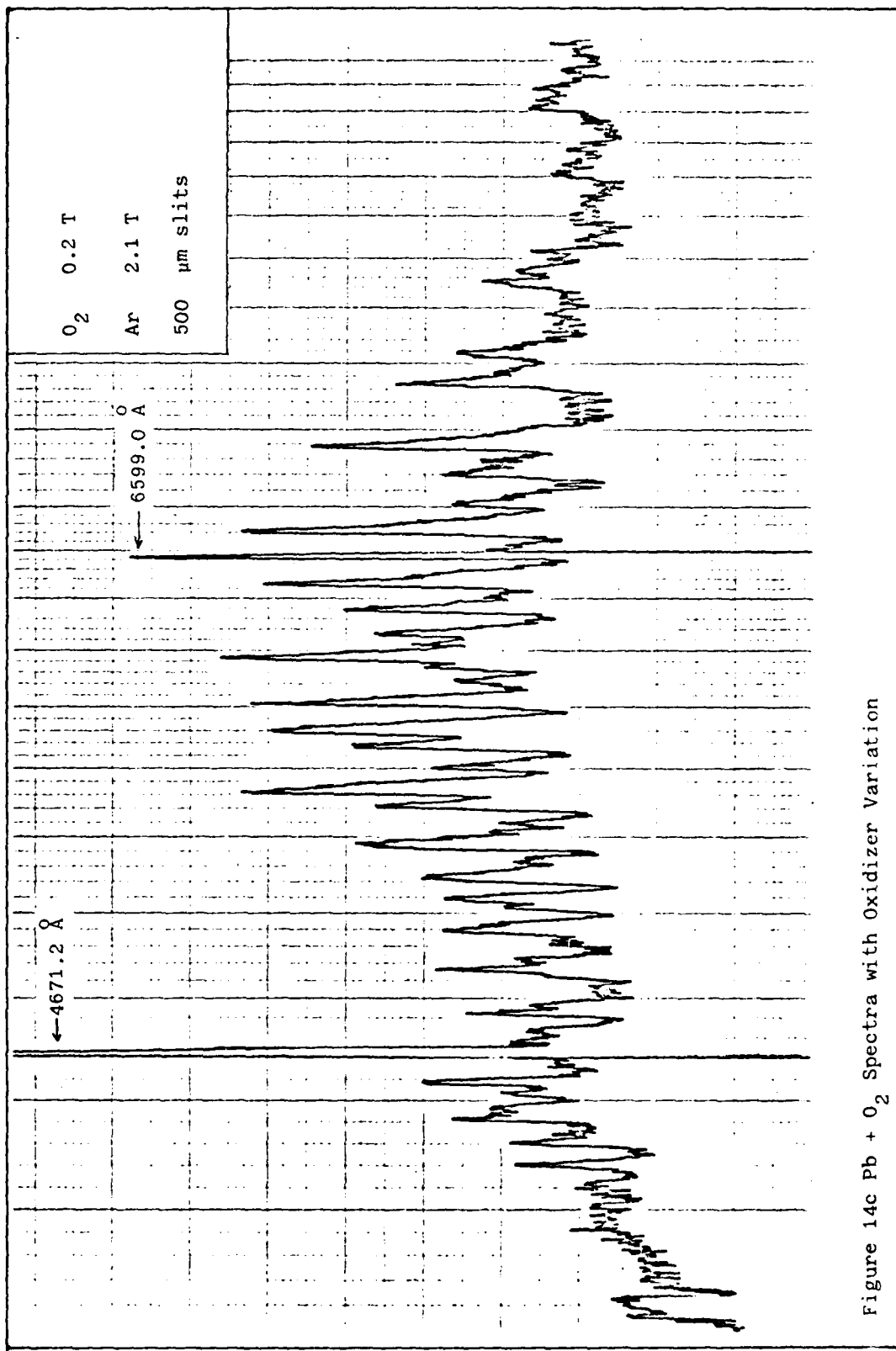


Figure 14c Pb + O<sub>2</sub> Spectra with Oxidizer Variation

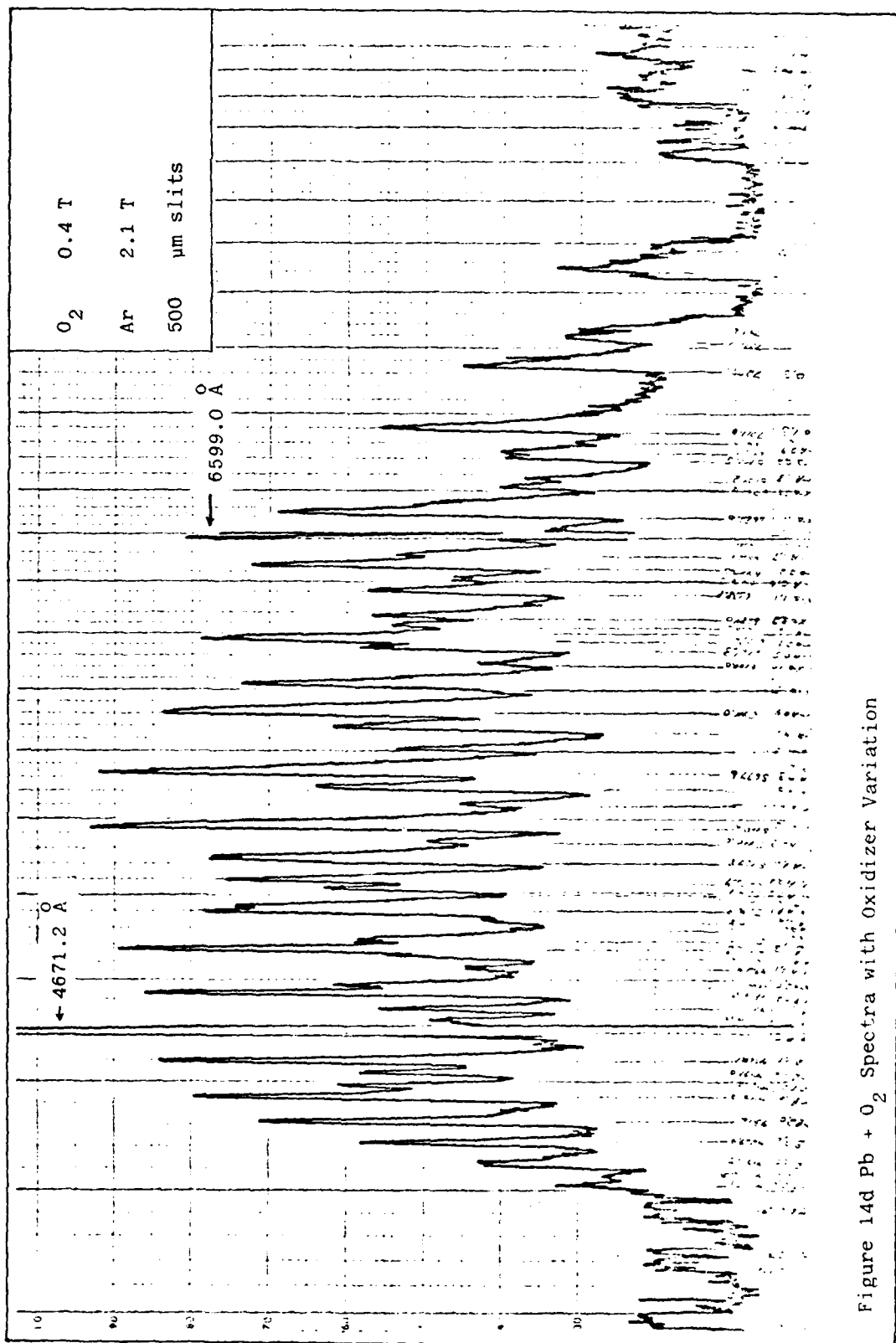


Figure 14d Pb + O<sub>2</sub> Spectra with Oxidizer Variation

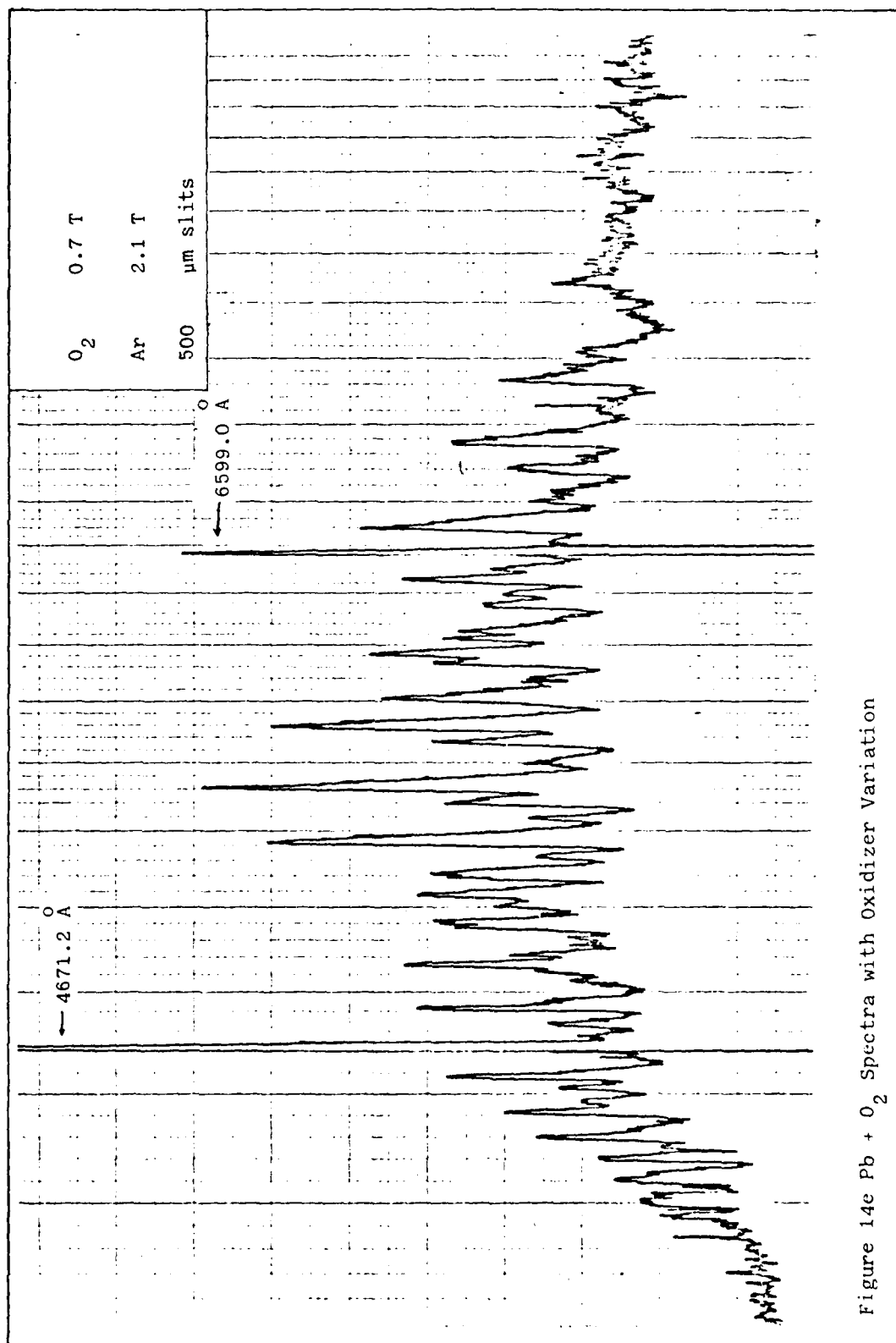
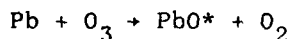


Figure 14e Pb +  $O_2$  Spectra with Oxidizer Variation

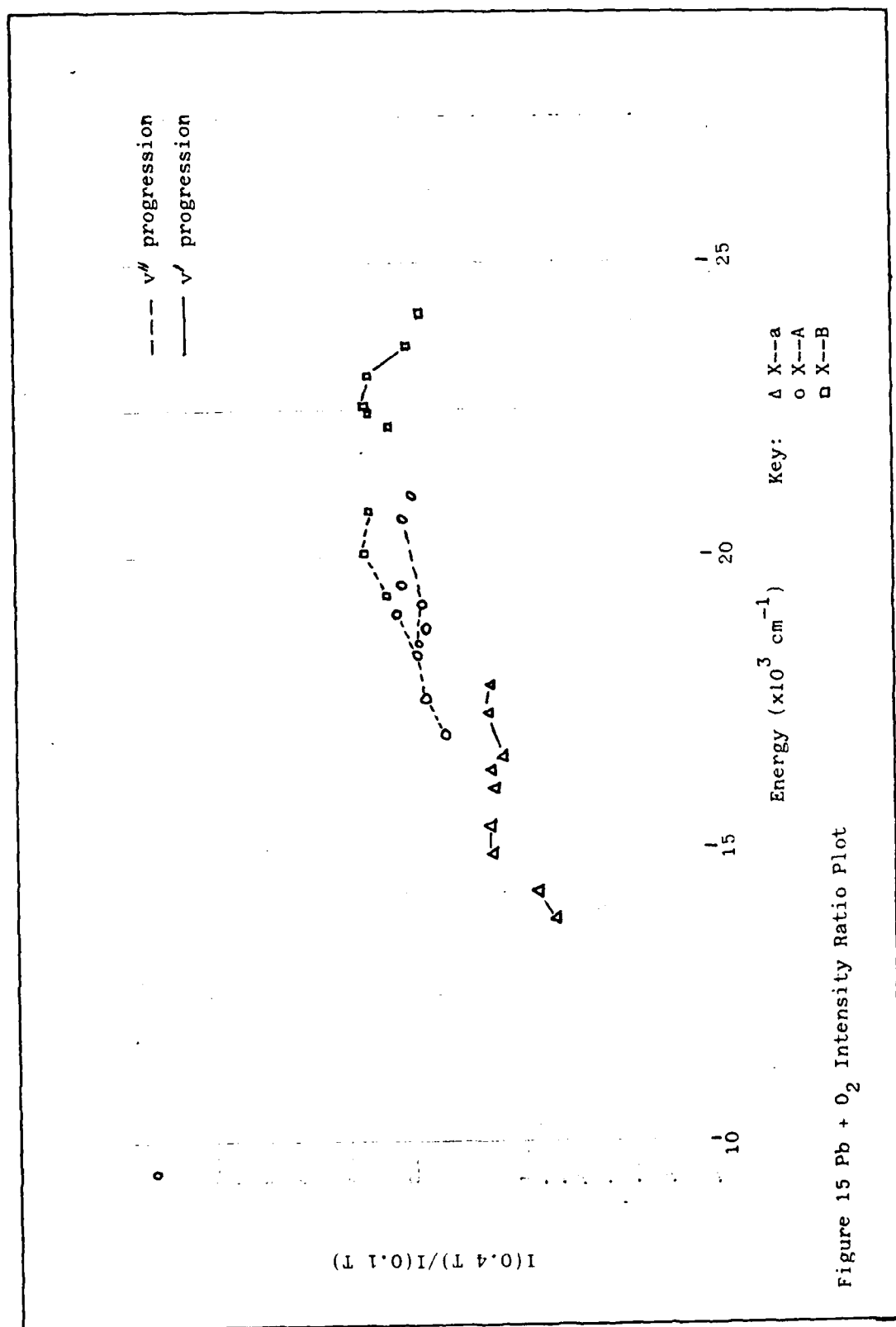
relative to the a state. Then, at 0.7 Torr, the strong enhancement of the B and A state had subsided and the spectra more closely resembled that observed at 0.1 or 0.2 Torr. Figure 13 shows a plot of the ratio of the emission intensity of different lines at 0.4 Torr to the intensity observed at 0.1 Torr versus energy above the ground state. From Figure 13 it can be concluded that line enhancements in the a state are relatively small with enhancement factors of 1.1 - 1.2 and some lines are even inhibited. Enhancement factors for the A state are between 1.6 and 2.2. The strongest enhancement occurs in emission from the B state. Here factors range from 1.8 - 2.7. The general trend of the data in Figure 15 is similar to Linton and Broida's results observed in the  $\text{Pb} + \text{O}_3$  reaction; see Figure 8a (6 percent  $\text{O}_3$  in  $\text{O}_2$ ). The pressures involved are also similar. This indicates that much of the emission observed by Linton and Broida's was actually due to the  $\text{Pb} + \text{O}_2$  reaction and not  $\text{Pb} + \text{O}_3$ . Also, the chemistry of the two reactions may be quite similar. Indeed, after the initial reaction,



the chemistry may proceed along the same lines. Although there is some degree of linearity in both the vibrational and electronic data the trends are not characteristic of a Boltzmann distribution.

A gradual increase or decrease in emission intensity from the excited states as pressure is varied is not unexpected. Indeed the intensity should reach a maximum at a point corresponding to the most efficient mixing of  $\text{O}_2$  and lead vapor. However, this does not explain why some states are enhanced more than others. The strong enhancement of the A and B state emission may be due to a collisional transfer mechanism. As the  $\text{O}_2$  pressure is increased the velocity of the  $\text{O}_2$  molecules



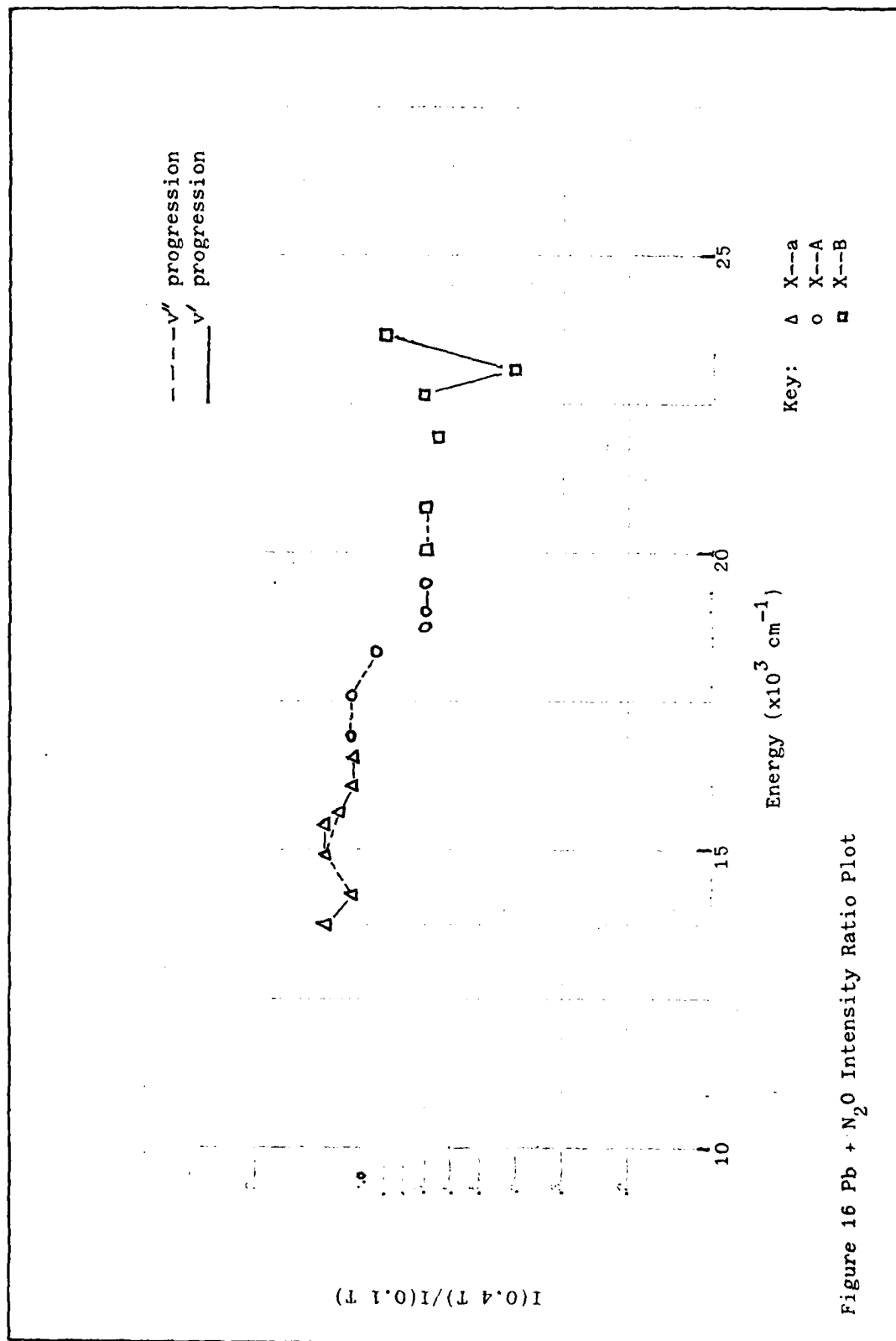


entering the flame will be greatly increased. Due to this increased velocity,  $O_2$  or  $O$  (from a secondary reaction) may have a greater cross section for reacting with the lead vapor. This increased cross section would tend to enhance the emission from a particular state. Linton and Broida found enhancement ratios 3-4 times higher for the A and B states in the  $Pb + O_3$  reaction than found here for the  $Pb + O_2$  reaction. This difference could be due to the presence of  $O_3$  or it could indicate a difference in the geometry of how the oxidizers are injected into the flame. The decrease in emission observed at 0.7 Torr could indicate the onset of reactions which quench the desired reactions at high pressures.

These results bear no similarity to Linton and Broida's  $Pb + O$  results. This is not surprising since the pressures used are so different and a large percentage of the  $O$  atoms were probably in excited states in Linton and Broida's work.

$Pb + N_2O$  Experiment. As in the  $Pb + O_2$  experiment, five spectra were taken in the region 3500 - 8700 Å. Argon pressure was maintained at 2.75 Torr throughout all the runs. The five oxidizer pressures were 0.05, 0.1, 0.2, 0.4 and 0.6 Torr. No dramatic enhancements of emission were observed. The actual plots of the spectra are shown in Appendix D. The ratios of the intensity of various lines at 0.4 Torr to that at 0.1 Torr is shown in Figure 16. The general trend of the data indicates that the emission from the a state increased slightly at higher pressure but that the A and B systems were generally inhibited at higher pressures. This agrees qualitatively with the Linton and Broida's results shown in Figure 8b. Although very little linearity is observed within the vibrational levels, the electronic states do seem to fall roughly in a linear fashion and could be described with a Boltzmann distribution. In this

experiment when the oxidizer pressure was increased to 0.6 Torr the emission observed changed dramatically. All systems were reduced in intensity. This suggests that the emission does not shift monotonically from blue to red (B and A to a) as pressure is increased but does so in a series of discrete increases and decreases. Recall that Linton and Broida found the a state emission significantly enhanced at a pressure of 34 Torr.



## VI. Conclusions and Recommendations

### Conclusions

A gas flow tube reactor has been used to generate a chemiluminescent flame from the reactions  $\text{Pb} + \text{N}_2\text{O}$  and  $\text{Pb} + \text{O}_2$ . The throughput of lead vapor from the furnace to the reaction region has been increased, resulting in more intense flames. This lead to better resolution because smaller slits could be used. The detection system has been optimized resulting in signal to noise ratios of 50 or 60 to 1 with 500  $\mu\text{m}$  slits. Emission was observed from five different electronic states. They were the a, b, A, B, and D states. Emission from the a state was generally the most intense, while that from the b state was weakest. The dependence of the chemiluminescent emission spectrum of PbO on changes in oxidizer pressure was studied at various oxidizer pressures below 1.0 Torr. Significant enhancement of emission from the B and A states was noted in the  $\text{Pb} + \text{O}_2$  reaction at 0.4 Torr of  $\text{O}_2$ . This low pressure enhancement mechanism has not been reported previously. The relative populations of the PbO electronic states can be roughly described by a Boltzmann distribution in the  $\text{Pb} + \text{N}_2\text{O}$  reaction at the pressures investigated. The severe fouling problems encountered by Linton and Broida in the  $\text{Pb} + \text{O}_2$  reaction were not encountered here. The reason for this is not clear. It is possible that small differences in the temperature of the lead vapor lead to dramatic differences in the chemistry involved. It could also be that the chemistry is much different at the higher pressures investigated by Linton and Broida. In this apparatus  $\text{Pb} + \text{O}_2$  would be the recommended reaction for studying emission from the a, A, and B states. The  $\text{Pb} + \text{O}_2$  reaction would probably be the most likely to exhibit a population inversion since the higher lying states are more heavily

populated. It is unlikely however than an inversion could be achieved without the introduction of some other excited species into the flame to serve as an energy transfer means.

#### Recommendations

Excited Gases. Excited gases, such as O,  $O_2(^1\Delta)$ ,  $N_2$  and  $NF_3$  should be introduced into the flame to determine if any of these can act as energy transfer agents to enhance emission from particular electronic states.

Flow Tube. The flow tube should be modified to assume the geometry shown in Figure 17. This geometry should greatly reduce the amount of coating which deposits on the observation windows. In the present flat geometry the reaction products impact the roof of the flow tube and spread out along the length of the tube. With the geometry shown in Figure 17 the reaction products will proceed directly toward the vacuum and filter and will not be recirculated through the tube body.

Chimney Design. Various chimney designs, based on the recommendations in Koyms thesis (Ref 15:65), should be investigated to determine which design yields the most efficient flow of lead vapor from furnace to reaction area.

Oxidizer Injection. The flow tube should be modified to permit the introduction of oxidizers well upstream of the flame. This will enable spectra to be taken at higher oxidizer pressures without the shape of the flame being severely altered.

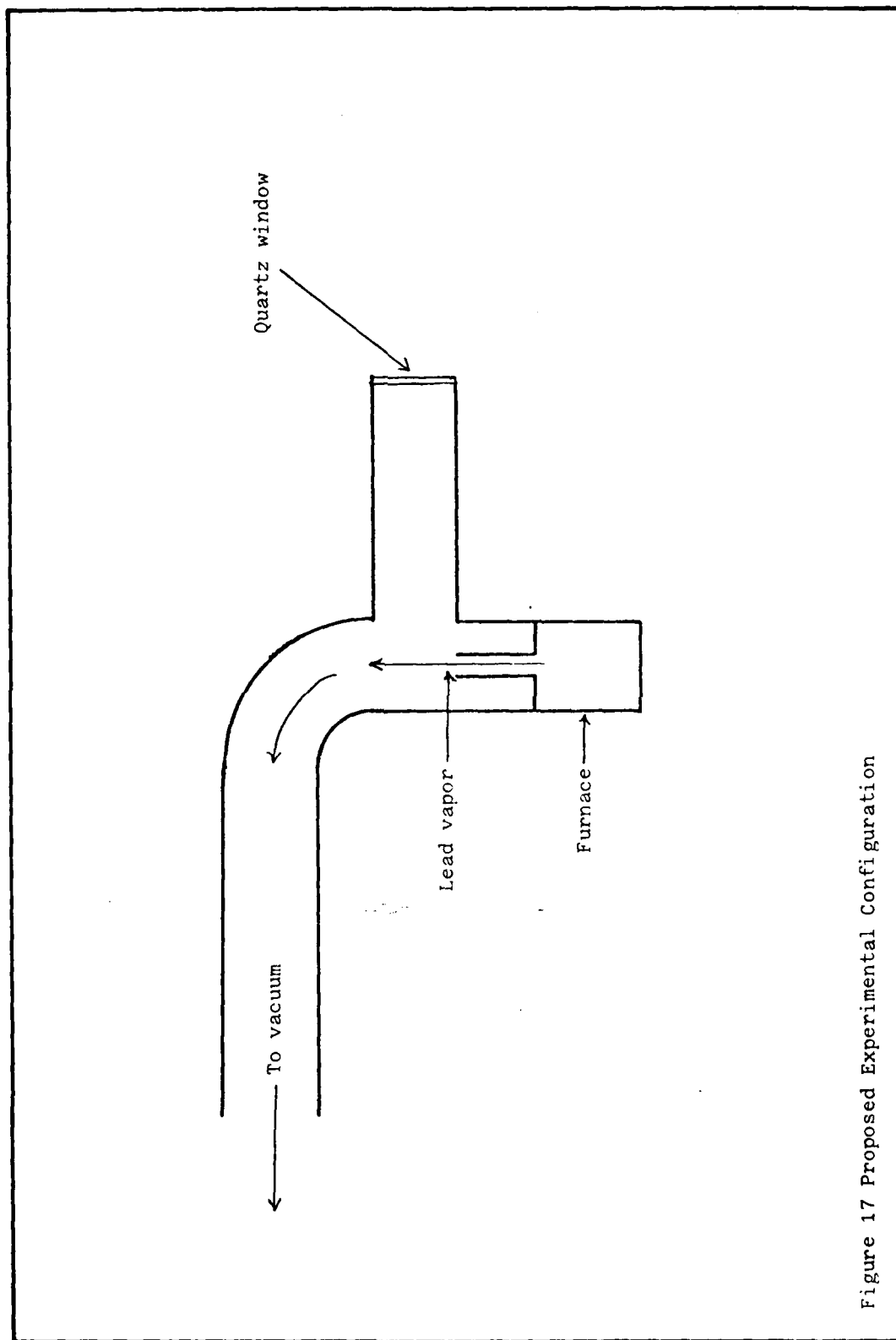


Figure 17 Proposed Experimental Configuration

### Bibliography

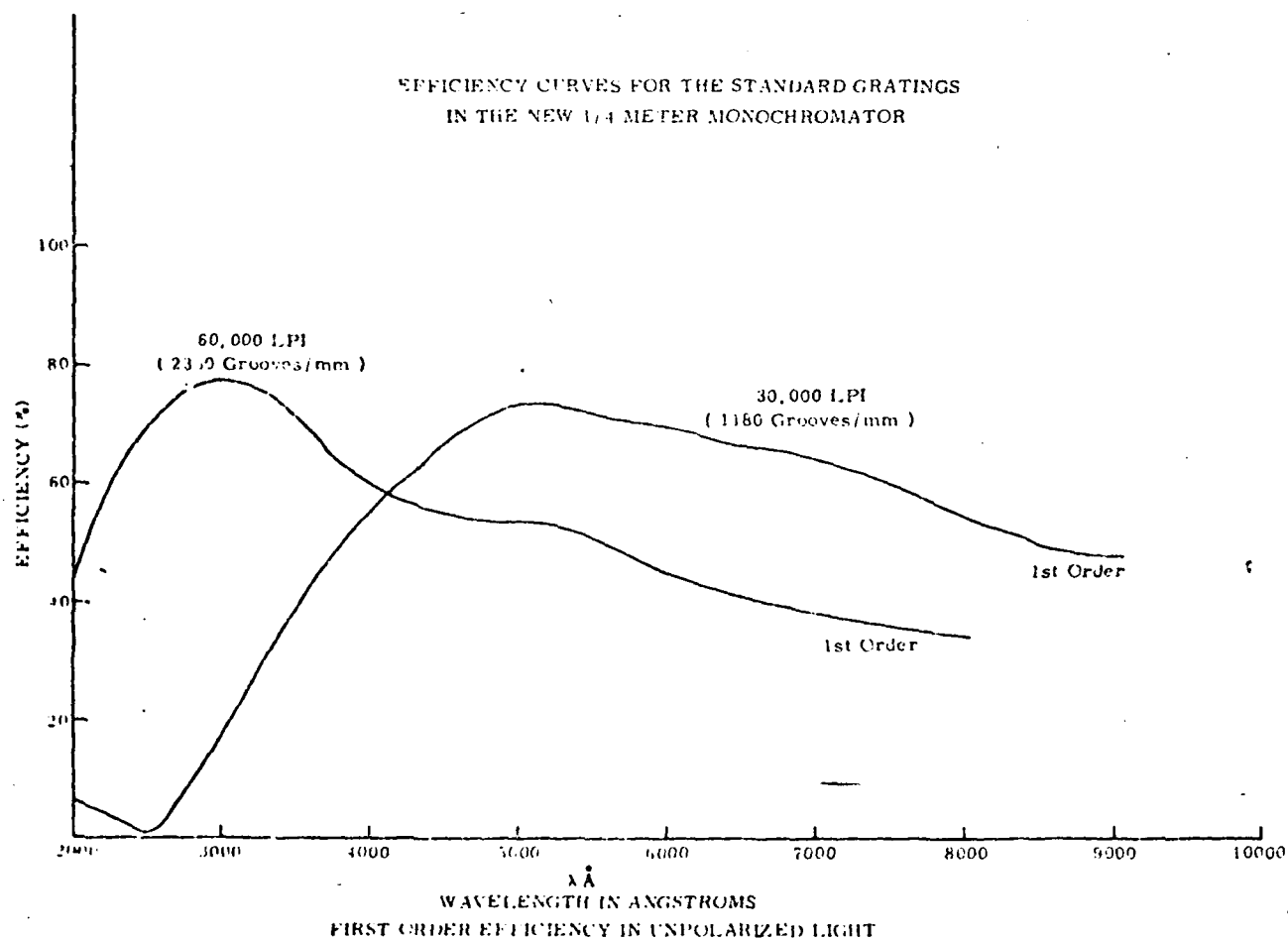
1. Steinfeld, Jeffrey. Molecules and Radiation. New York: MIT Press, 1978.
2. Herzberg, G. Spectra of Diatomic Molecules, (Second Edition): New York: Reinhold Co., 1950.
3. Linton C. and H. P. Broida. "Chemiluminescent Spectra of PbO from Reactions of Pb Atoms." Journal of Molecular Spectroscopy, 62: 395-415 (September 1976).
4. Oldenberg, R. C., et al. "A New Electronic Band System of PbO." Journal of Molecular Spectroscopy, 58: 283-300 (November 1975).
5. Kurylo, M. J., et al. "A Study of the Chemiluminescence of the Pb + O<sub>3</sub> Reactions." Journal of Research of the NBS, 80A, No. 2: 167-171 (March-April 1976).
6. West J. B., et al. "Flow System for the Production of Diatomic Metal Oxides and Halides." Review of Scientific Instruments, 46: 164-168 (February 1975).
7. Nair, K. P. R., et al. "Potential Energy Curves and Dissociation Energies of Oxides and Sulfides of Group IVA Elements." Journal of Chemical Physics, 43: 3570-3574 (November 1965).
8. Bloomenthal, S. "Vibrational Quatum Analysis and Isotope Effect for the Lead Oxide Band Spectra." Physical Review, 35: 34-45 (January 1930).
9. Barrow, R. F., et al. "Rotational Analysis of the Absorption Spectrum of PbS." Proceedings of the Physics Society of London, 81: 697-704 (April 1963).
10. Brom J. M., Jr., and Beattie, W. H., "Laser Excitation Spectrum of PbO." Journal of Molecular Spectroscopy, 81: 445-454 (March 1980).
11. The Oxide Handbook, edited by G. V. Samsonon. New York: Plenum, 1973.
12. Fontijn, A. and W. Felder. "High Temperature Fast-Flow Reactor Study of Sn/N<sub>2</sub>O Chemiluminescence." Chemical Physics Letters, 34: (2): 398-402 (May 1972).
13. Handbook of Chemistry and Physics, (Fifty-fourth edition). Cleveland: The Chemical Rubber Company, 1973.



14. Thermo-Chemical Tables, Second Edition. USDC-NBS, JANAF  
Washington D.C.: National Bureau of Standards, 1971.
15. Koym, Raymond V. A Gas Flow Tube for Spectroscopic Studies.  
MS Thesis, Wright-Patterson AFB, OH: Air Force Institute of  
Technology, December 1980.
16. Sax, N. I. Dangerous Properties of Industrial Material, Third  
Edition. New York: Reinhold Press, 1968.
17. Suchard, S. N. Spectroscopic Data for Heteronuclear Diatomic  
Molecules, Volume II, Plenum Publicationa, 1975.

Appendix A

Grating Response Curves<sup>1</sup>



1. Taken directly from Jarrell Ash Manual

## Appendix B

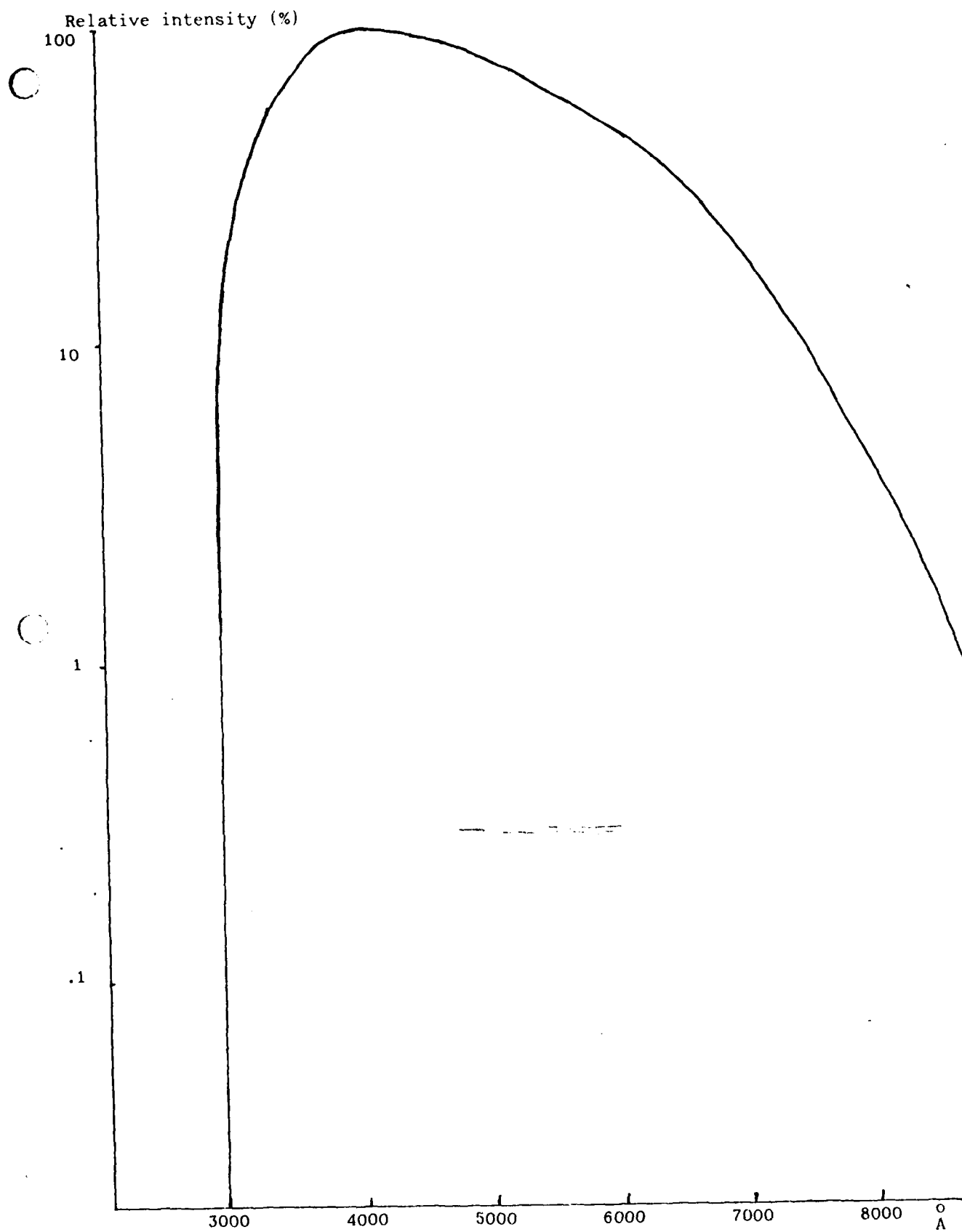
### Photomultiplier Response Curve<sup>1</sup>

This appendix gives important photomultiplier tube data and a graph of the tube's spectral sensitivity Graph values may vary  $\pm 10\%$ .

#### RCA 7265

Typical anode sensitivity @ 4200A <sup>o</sup> -----	$3.0 \times 10^6$ A/W
Typical cathode sensitivity @ 4200A <sup>o</sup> -----	0.064 A/W
Current amplification-----	$4.8 \times 10^7$
Anode dark current-----	$5.0 \times 10^{-8}$ A
Equivalent anode dark current input-----	$1.2 \times 10^{-13}$ W
Equivalent noise input-----	$2.1 \times 10^{-15}$ W

1. Taken from RCA Tube Handbook, HB-3. Harrison NJ: 1967

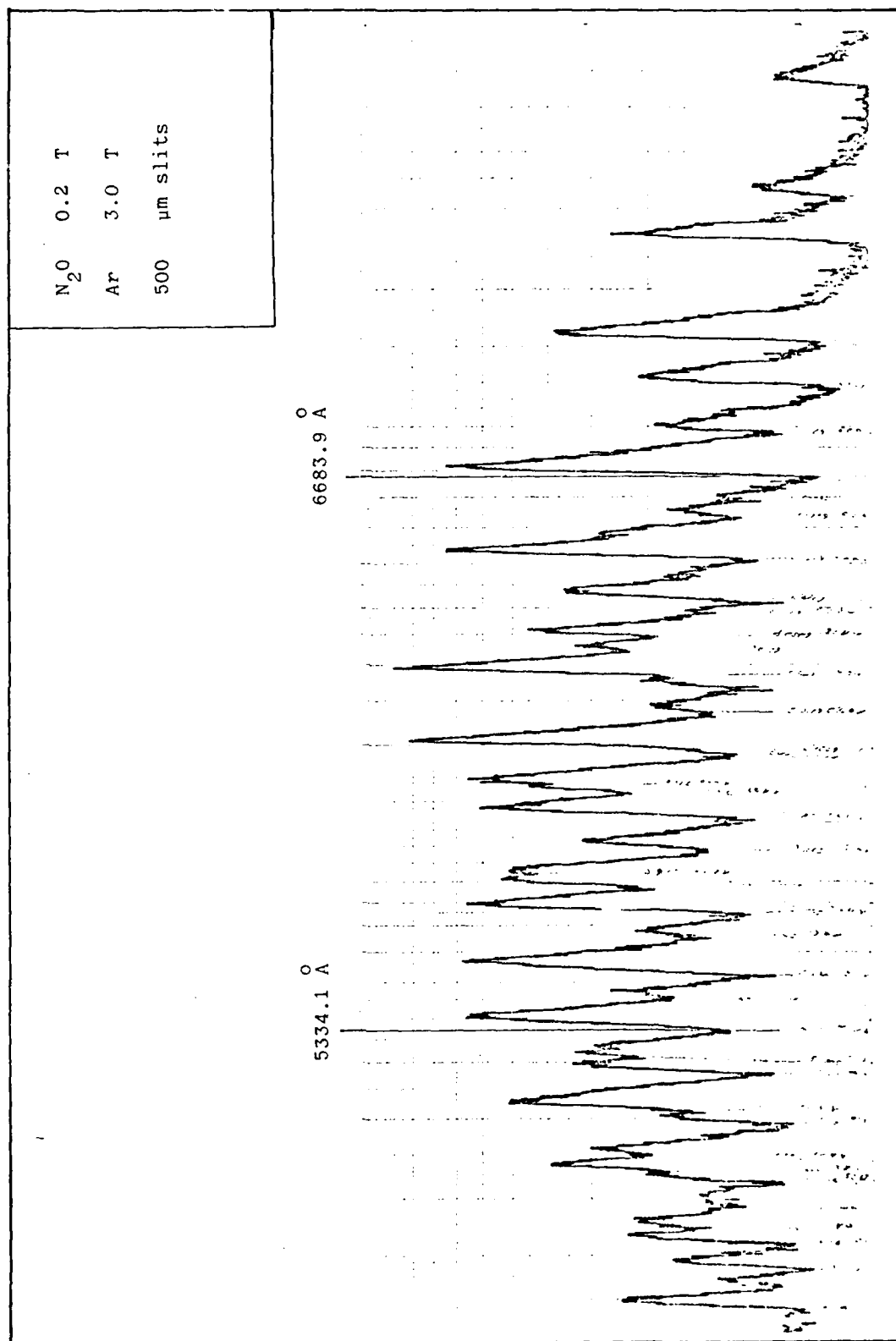


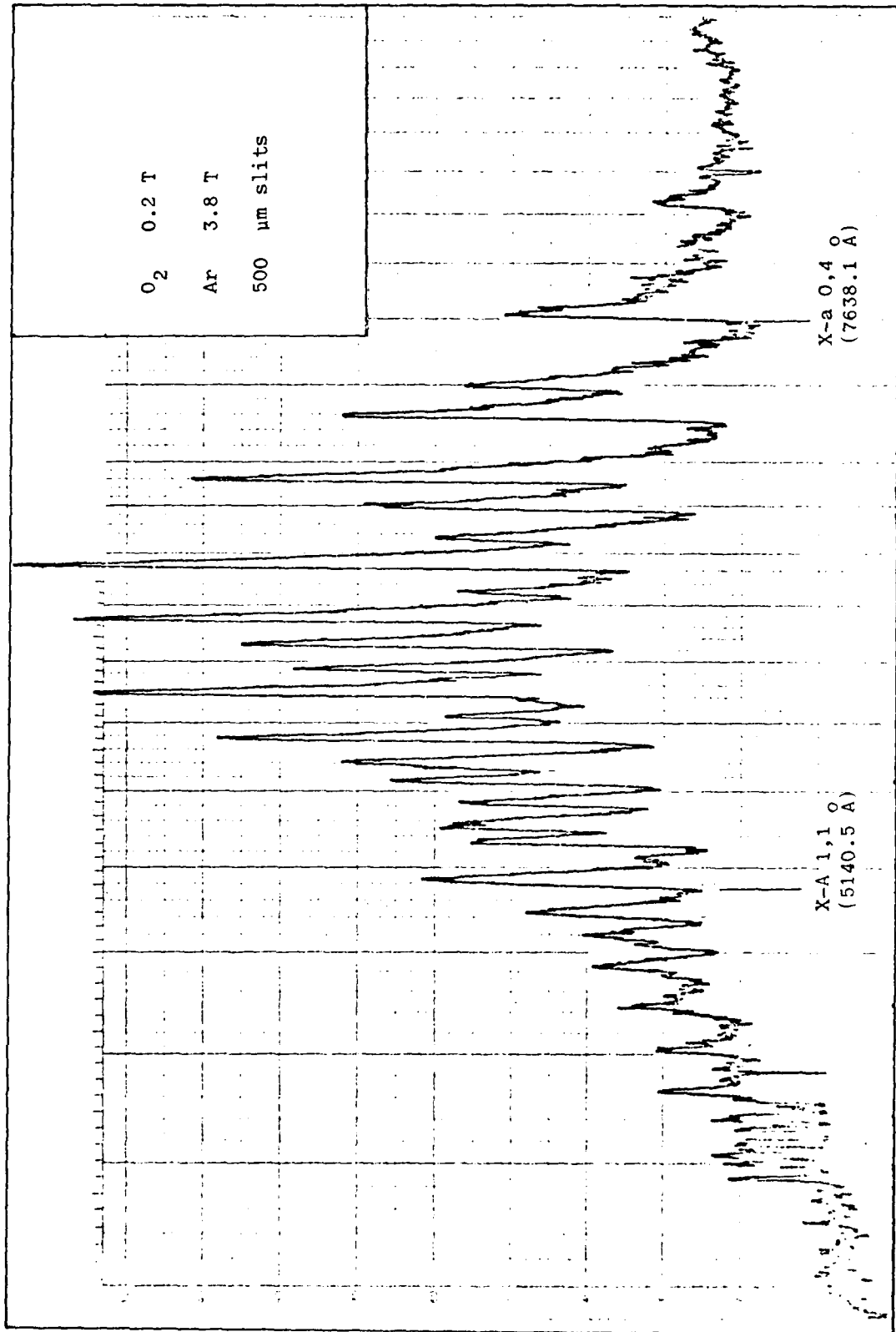
C

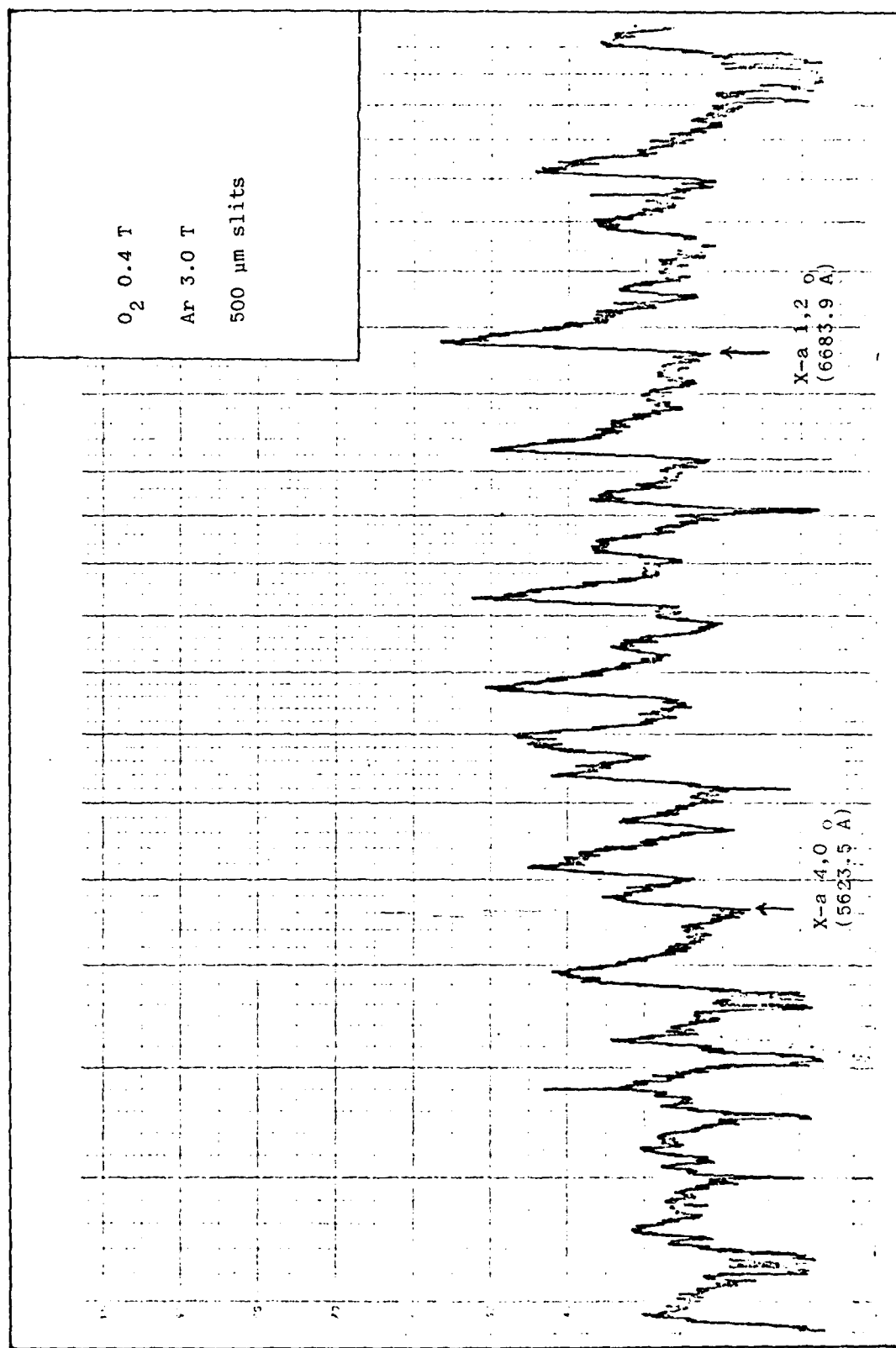
Appendix C  
Representative Spectra

Shown on the following pages are spectra typical of those obtained during this research. These are shown merely to give the reader a better idea of how the raw data appeared.

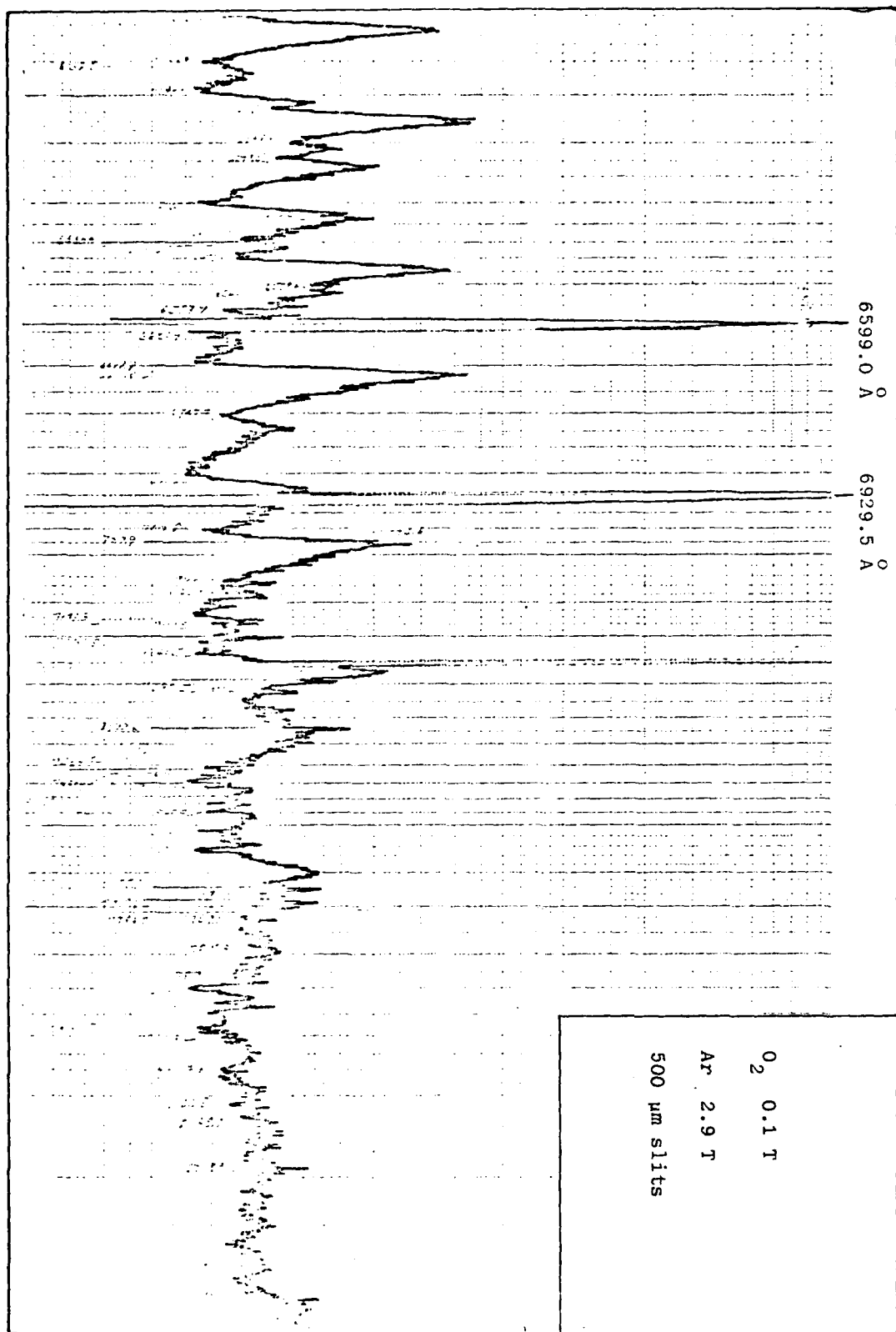
1 C

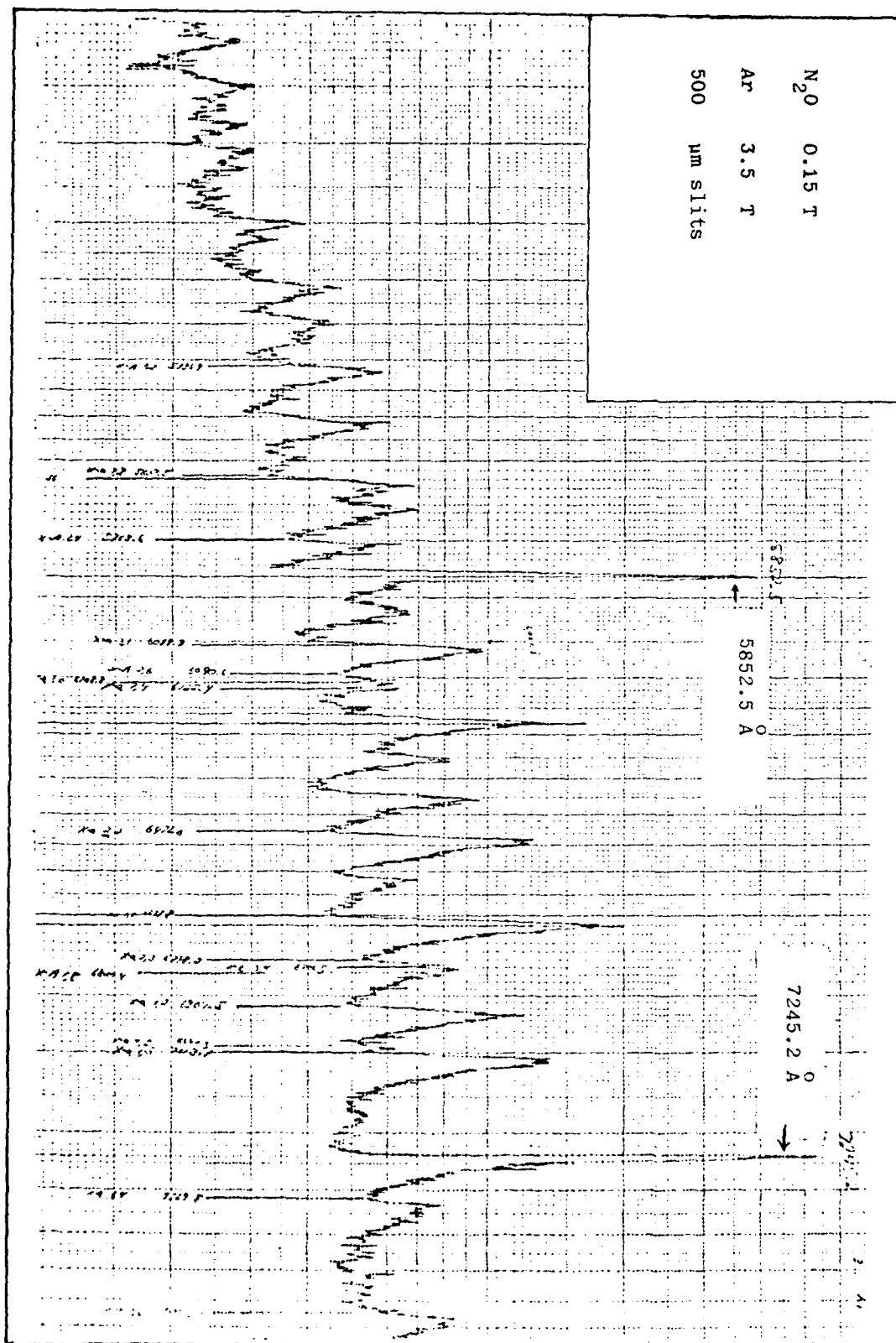








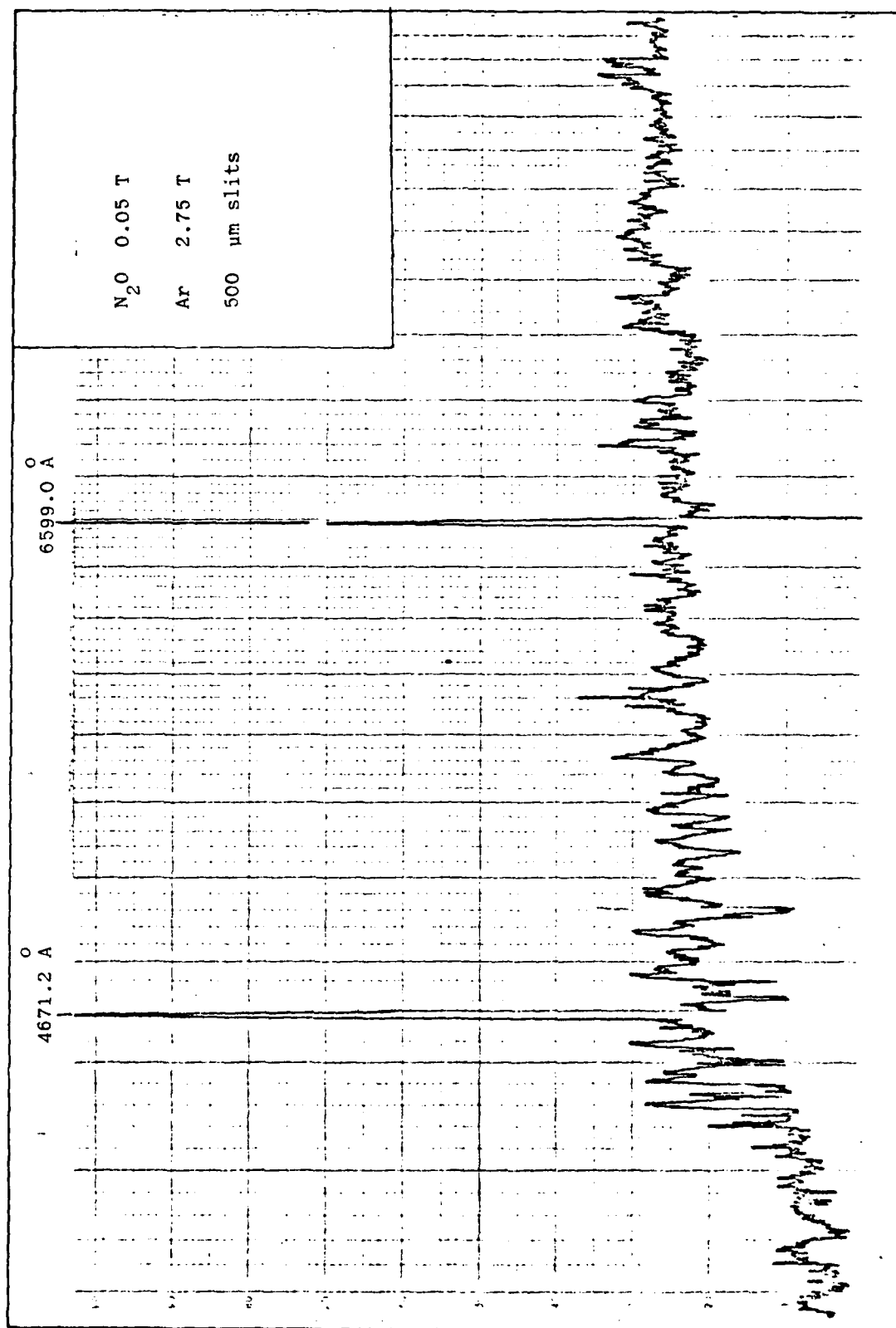


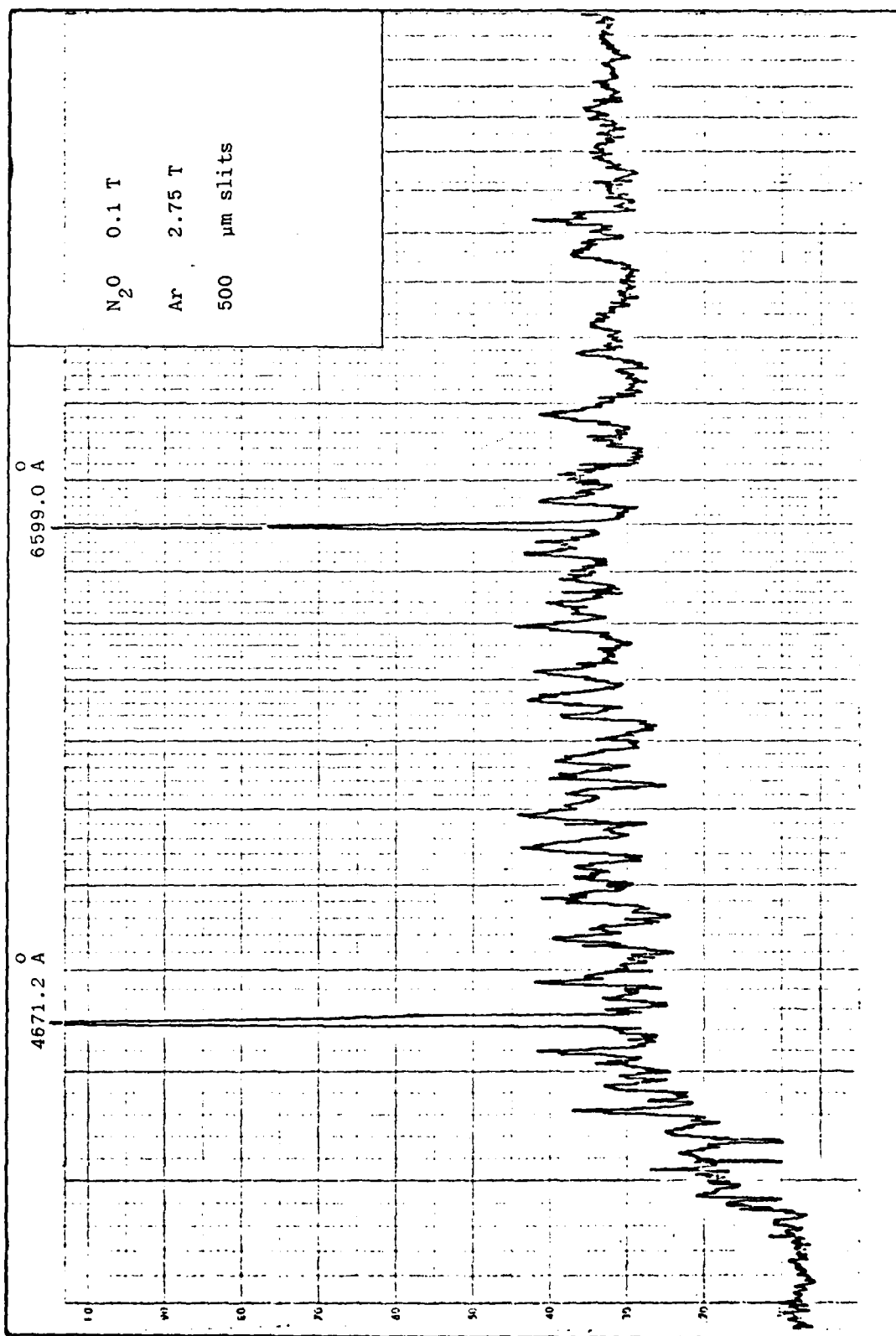


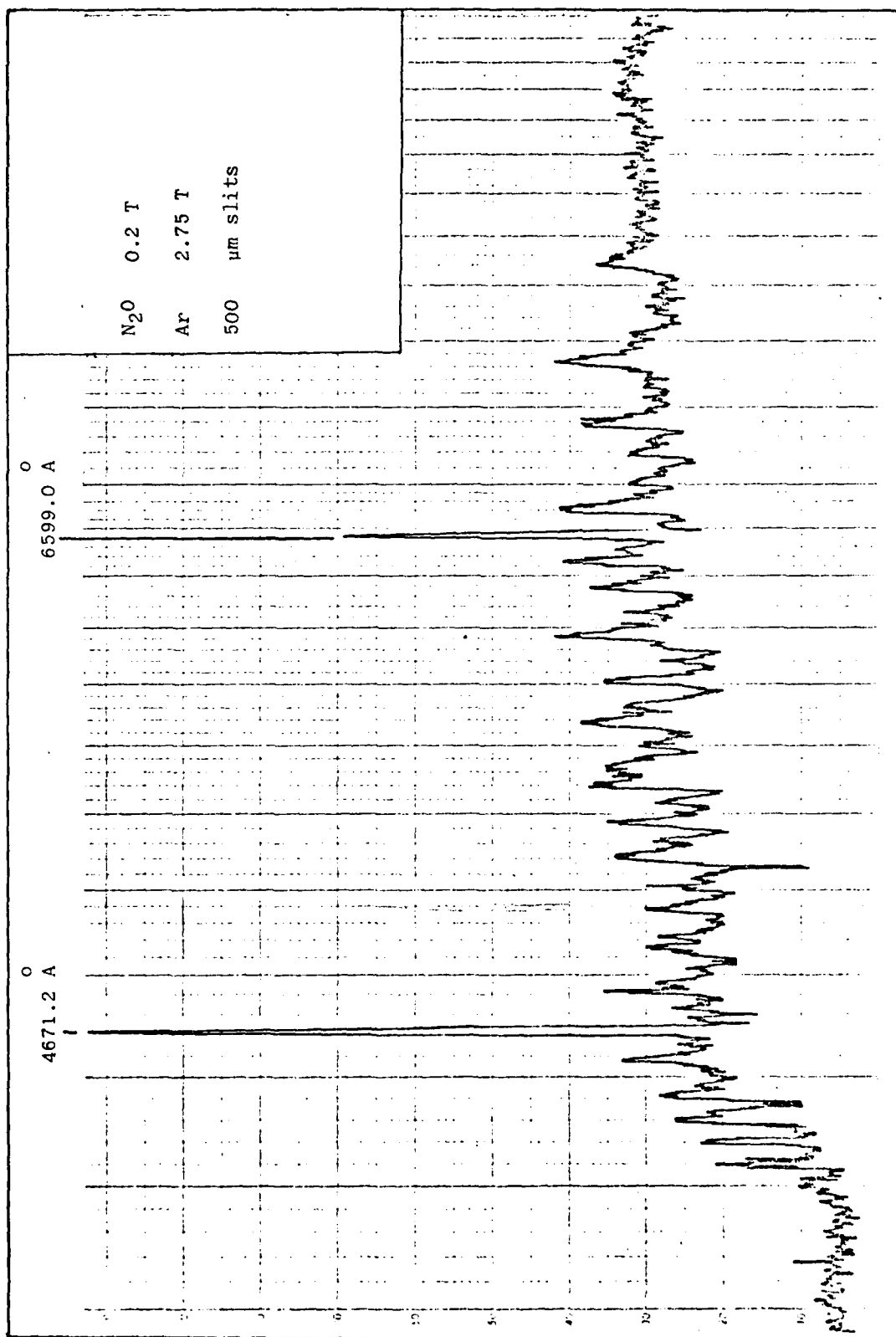
Appendix D

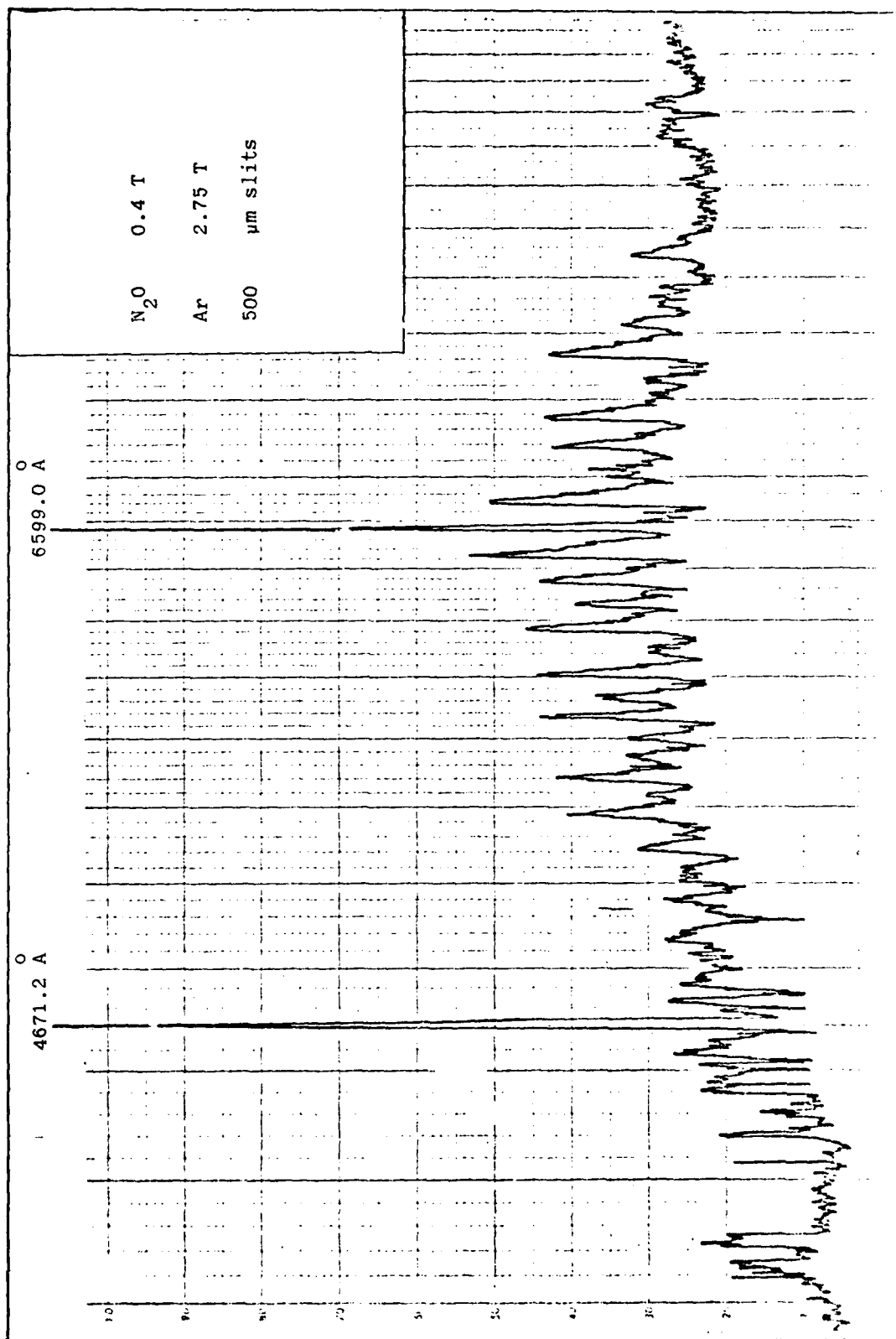
Pb + N<sub>2</sub>O Pressure Variation Spectra

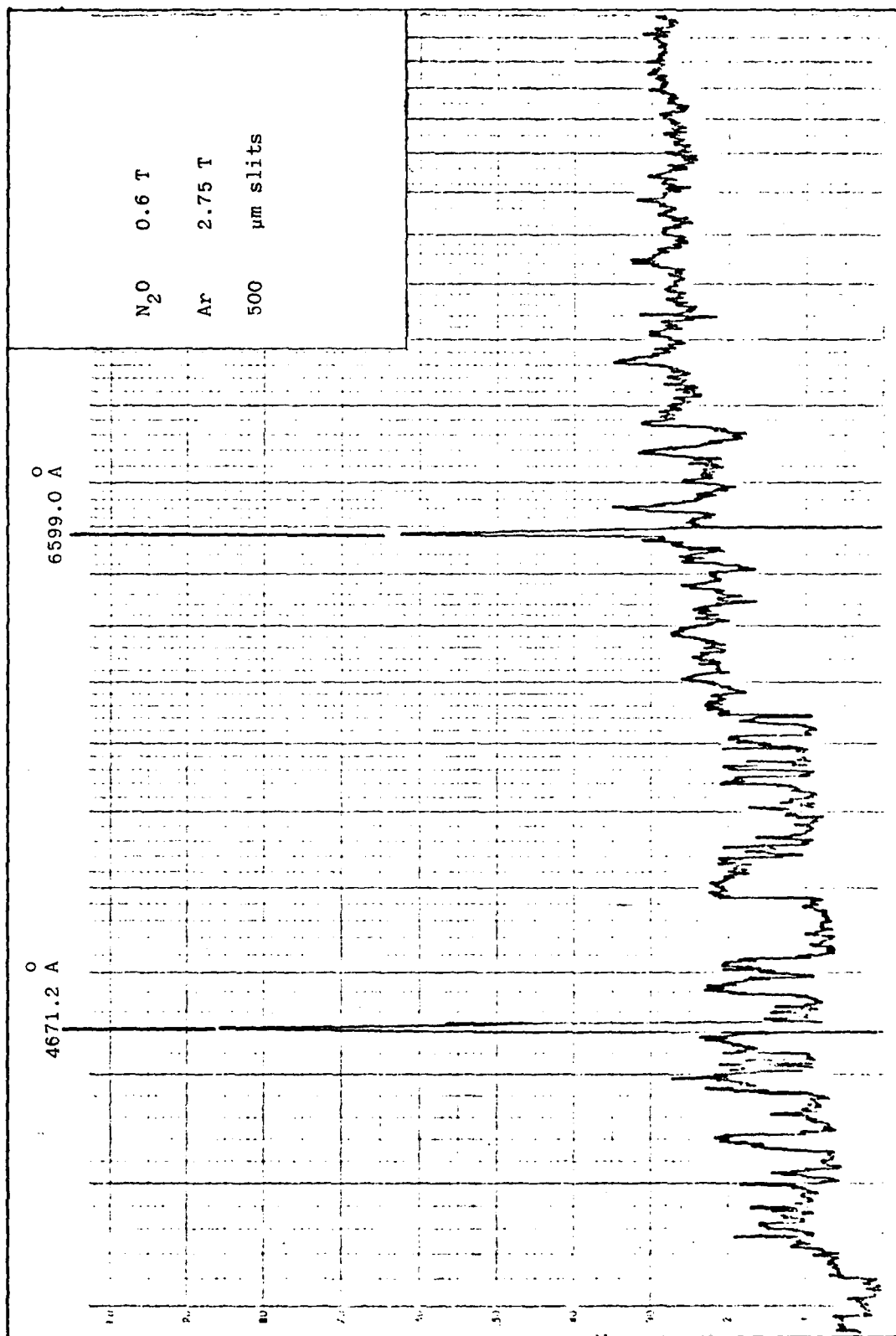
The following five pages shown the spectra which were obtained for the Pb + N<sub>2</sub>O reaction as the N<sub>2</sub>O pressure was varied from 0.05 to 0.6.













### Vita

Steven Richard Snyder was born on September 30, 1955 in Ft. Worth, Texas. He graduated from high school in Ashtabula, Ohio in 1974. He entered the United State Air Force Academy the same year and graduated in 1978. Upon graduation, he was assigned to the Foreign Technology Division on Wright-Patterson AFB where he was employed as a scientific intelligence analyst for two years. He entered the Air Force Institute of Technology in 1980 enrolled in the Engineering Physics program.

Permanent address: 1228 Van Winkle Drive  
Ashtabula, Ohio 44004

SECURITY CLASSIFICATION OF THIS PAGE (When Data Entered)

DD FORM 1473 EDITION OF 1 NOV 65 IS OBSOLETE

SECURITY CLASSIFICATION OF THIS PAGE (When Data Entered)

UNCLASSIFIED

SECURITY CLASSIFICATION OF THIS PAGE (When Data Entered)

BLOCK 20: Abstract (Cont'd)

different oxidizers were compared. Significant differences in spectral line intensities were recorded. The pressure dependence of the intensities was also measured. Again, significant differences were recorded when the two different oxidizers were used. In the  $Pb + O_2$  reaction a low pressure enhancement of various lines was observed. Significant differences between the chemistry of these low pressure reactions and the chemistry of similar reactions of high pressure were observed.

UNCLASSIFIED

SECURITY CLASSIFICATION OF THIS PAGE (When Data Entered)

**DAT  
FILM**